Novel gut probiotic engages microbiota for recovery and pathobiont clearance while preventing inflammation

Authors: Vitor Cabral[1,*†], Rita A. Oliveira[1,3,*†], Margarida B. Correia[1], Miguel F. Pedro[1,4], Carles Ubeda[2], Karina B. Xavier[1,†]

Affiliations:

[1]Instituto Gulbenkian Ciência, 2780-156 Oeiras, Portugal

[2]FISABIO, Valência, Spain

[3]Current address: Duchossois Family Institute, The University of Chicago, Chicago, IL, USA

[4]Current address: LEAF, TERRA, Instituto Superior de Agronomia, University of Lisbon, Portugal

* These authors contributed equally and share co-first authorship of this publication

[†]To whom correspondence should be addressed:

vcabral@igc.gulbenkian.pt; kxavier@igc.gulbenkian.pt; aaoliveira@uchicago.edu

Keywords: gut microbiota; recovery; colonization resistance; probiotic; *Klebsiella*; inflammatory bowels disease; butyrate; inflammation; intestinal pathogens; *Escherichia coli*; AIEC; *Enterobacteriaceae*

Abstract

Intestinal inflammation is at the root of several acute and chronical diseases, many times with unclear etiology where the gut microbiota, genetic predisposition, and/or environmental conditions all play a role. Its recurrence locks patients in long-lasting disease cycles that greatly diminish quality of life and might lead to life-threatening conditions.

Current treatments focus on attenuation of inflammatory episodes, through antibiotics or anti-inflammatory medication. However, while mitigating inflammation, such therapies also promote major changes in the intestinal microbiota with consequent loss of its beneficial functions, such as protection against pathogenic bacteria, leading to infections that can reactivate intestinal inflammation, resulting in relapse. Alternative and complementary treatments that can break the inflammation-treatment-infection-inflammation cycle are urgently needed as the next therapeutic breakthrough for intestinal inflammatory conditions.

Here, we use an Inflammatory Bowel Disease (IBD) model that is susceptible to inflammatory episodes to demonstrate how the use of a protective native gut commensal bacterium can break the disease cycle.

Our probiotic therapy, centered of the gut commensal bacterium *Klebsiella* sp. ARO112, can transiently colonize an imbalanced and infected microbiota, preventing the relapse of intestinal inflammation, by promoting a faster recovery of the gut microbial community. This ARO112-induced recovery is driven by the resurgence of native bacteria and butyrate production, halting the relapse of inflammation, and displacing the pathobiont Adherent and Invasive Escherichia coli (AIEC), thereby halting the disease cycle by avoiding the need for further treatments.

This promising biotherapy could be used to break the inflammation-treatment-infection-inflammation cycle that traps most not only IBD patients, but also in many other inflammatory based conditions, allowing for their gut microbiota to recover from debilitating diseases and increasing their quality of life.

48 **Introduction**

49 The gut microbiota plays a crucial role in human health and disease. An abundant and diverse
50 intestinal community of microorganisms performs essential functions, including providing colonization
51 resistance to potential pathogenic external bacteria. This protective capacity can be significantly
52 compromised by environmental perturbations that alter the population composition, such as changes in diet
53 or medical treatments, like antibiotics [1]–[3]. These shifts in populational dynamics, induced by dietary
54 changes and antibiotic treatments, can be challenging to rectify, leaving patients more susceptible to
55 infections and other medical complications [4].

56 The pursuit of interventions to restore dysbiotic gut microbiotas has gained momentum. Currently,
57 both basic research and clinical studies encompass a range of approaches, from introducing single protective
58 bacterial species to well-defined bacterial communities or even complete microbiota, as in fecal microbiota
59 transplants (FMT) [5]. Although the United States Food and Drug Administration has recently approved FMT
60 for the successful treatment of recurrent *Clostridioides difficile* infections in humans [6], the undefined nature
61 of these procedures poses safety risks [7], [8]. These risks underscore the need for the identification of
62 defined strategies, which could involve either single- or multi-strain bacterial cocktails. Next-generation
63 probiotic bacteria, defined as bacterial species native to the host, which upon ingestion and/or colonization,
64 provide benefits to the host, offer promise for restoring microbiota functions. This requires an extensive
65 understanding of the benefits, potential drawbacks, and the organism's safety profile, all of which are
66 important to its therapeutic importance.

67 Patients with high susceptibility to infections often undergo extensive antibiotic treatments,
68 rendering them more susceptible to recurrent infections. These patients require innovative approaches to
69 complement current treatments and break the cycle of disease recurrence. Inflammatory Bowel Diseases
70 (IBD) are a group of multi-factorial pathologies with a complex etiology, where genetic predisposition, gut
71 microbiota, and environmental conditions play a role [9]. Three outcomes emerge as key aspects of disease
72 cycles that afflict IBD patients: gut microbiota imbalances [10], increased and persistent intestinal
73 inflammation [11], and susceptibility to intestinal infections [12]. To manage inflammation flares, IBD
74 patients are often prescribed antibiotics or anti-inflammatory medication [13]. However, these treatment
75 options can inadvertently harm the microbiota, often exacerbating the proinflammatory intestinal
76 environment [14], thus perpetuating the cycle. The consequent loss of natural protection provided by a
77 balanced microbiota often leads to infections by *Enterobacteriaceae* bacteria, like the adherent-invasive
78 *Escherichia coli* (AIEC), which can also trigger inflammatory episodes [15].

79 Probiotics are often considered as potential alternative or complementary treatments for intestinal
80 diseases, but their benefits for complex pathologies like IBD have been limited [16]. *E. coli* Nissle 1917 has

been proposed as a potential therapy for IBD [17]. However, despite various proposals and even clinical trials [18], the European Society for Clinical Nutrition and Metabolism, recommends against probiotics for treatment nor prevention of Crohn's Disease [19], owing to lack of promising results obtained thus far. Therefore, therapeutic probiotics warrant further research, as their efficacy in patients has been inconsistent [20]–[23].

In previous work, we have identified a commensal intestinal bacterium, *Klebsiella* sp. ARO112 from the *Enterobacteriaceae* family. ARO112 provides partial colonization resistance against an invading *Escherichia coli* K-12 MG1655 strain and *Salmonella enterica* Typhimurium in a streptomycin-induced intestinal dysbiosis murine model [24]. ARO112 can also displace the invader *E. coli*, when administered as a treatment, i.e., after colonization by the invading *E. coli*, in the presence but also in the absence of other microbiota members (in ex-germ-free mice). The ability to displace an already established bacterial invader is not a standard feature, even among probiotic strains. Research has shown that commercially available probiotics can partially displace certain pathogenic bacteria but with varying efficacy [25]. Our previous findings have prompted us to test the potential of ARO112 strain as a next-generation probiotic, capable of delaying or eliminating colonization by other *Enterobacteriaceae* invading the gut community during dysbiotic events.

In this study, we assessed the safety of ARO112 strain by evaluating its pathogenic potential for an assembly of pathogenic traits commonly associated with *Enterobacteriaceae* clinical isolates. Our results show that ARO112, compared to other well-characterized *Enterobacteriaceae,* has low pathogenic potential, limited efficiency in acquiring or maintaining plasmids carrying antibiotic resistance, and does not induce host inflammation, unlike *E. coli* Nissle 1917. Simultaneously, ARO112 displayed a competitive advantage for colonization against different species from the Pseudomonadota phylum (formerly known as Proteobacteria). Its competitive properties and lack of inflammatory potential had a significant impact in an IBD mouse model, where ARO112 exhibited strong potential as a next-generation probiotic, reducing infectious bacterial loads, preventing gut inflammation, and promoting butyrate-producing microbiota recovery from antibiotic-induced dysbiosis.

113 **Results**

114 **ARO112 encodes fewer predicted pathogenic traits when compared with other *Enterobacteriaceae***

115 To address the potential of ARO112 as a probiotic, we performed a genome comparison analysis with
116 fifteen *Enterobacteriaceae* strains to assess their pathogenic potential, including five *E. coli* strains, five
117 *Klebsiella pneumoniae* strains, and five non-*pneumoniae Klebsiella* strains, including ARO112 (Supplementary
118 table 1). These strains were selected in order to incorporate human (clinical) and murine bacterial isolates,
119 including pathogenic, commensal, and one established probiotic strain, as well as type or laboratory strains
120 for these groups. With this broad strain selection, we expected to involve a wide range of encoded virulence
121 traits and bacteria with different pathogenic potential.

122 A whole genome-based phylogenetic tree segregates the fifteen strains into three major clades,
123 differentiating among *E. coli*, *K. pneumoniae*, and non-*pneumoniae Klebsiella* strains (Fig. 1a). The non-
124 *pneumoniae Klebsiella* clade shows *Klebsiella* sp. ARO112 clustering with *Klebsiella grimontii* (Kgr) type strain
125 and close to *K. michiganensis* (Kmi) type strain, and *Klebsiella oxytoca* MBC022 mouse commensal clustering
126 with the *K. oxytoca* DSM5175 (Kox) type strain. This placement of *Klebsiella* sp. ARO112 closer to Kgr than
127 Kmi had already been shown by others [26], [27], where ARO112 was compared to other non-*pneumoniae*
128 *Klebsiella* strains isolated from humans. Osbelt and colleagues have shown that ARO112 strain is close, but
129 not part of, the cluster of 3 *K. grimontii* tested [26], raising the hypothesis that ARO112 might not be a *K.*
130 *grimontii* species. In the *E. coli* clade, the probiotic *E. coli* Nissle 1917 (EcN) and the pathobiont AIEC (LF82)
131 strains were phylogenetically closer to each other than to both non-pathogenic *E. coli* K-12 (MG1655) and *E.*
132 *coli* B (EcB) laboratory strains and to the multi-resistant clinical isolate *E. coli* (Ec1898) (Fig. 1a). In the *K.*
133 *pneumoniae* clade, the three clinical isolates cluster together (MH258, Kp1012, and Kp834), while the other
134 two Kpn strains (NCTC9633 and ATCC43816) form a distinct cluster.

135 To predict the genome-encoded pathogenic potential of these strains we resorted to 9 databases
136 reported in Bacterial and Viral Bioinformatics Resource Center [28] for virulence factors, drug targets and
137 transporters, and antibiotic resistance genes. The presence/absence of the pathogenic properties segregated
138 the three clades represented in the phylogenetic tree (Fig. 1b,c). We analyzed the pathogenic properties that
139 are ubiquitous (present in all 5 strains) or non-ubiquitous (not present in all 5 strains) of each group
140 (Supplementary Table 2). In the non-*pneumoniae Klebsiella* strains, there are 64 absent properties when
141 compared to *K. pneumoniae* strains, of which 48% encode for transporters and membrane proteins,
142 indicating an overall lower pathogenic potential predicted for the non-*pneumoniae Klebsiella* group. The
143 difference in absent predicted virulence properties of the non-*pneumoniae Klebsiella* strains was even higher
144 when compared with *E. coli* strains (403), which mainly included genes encoding for transporters, membrane
145 proteins, and genes potentially conferring resistance to antibiotics (Fig. 1b, Supplementary Table 2). There

146 are other properties absent in the non-*pneumoniae Klebsiella* strains, but present in the *E. coli* strains that
147 are notable, such as genes related to lipopolysaccharide (LPS) biosynthesis and assembly, flagellum, type IV
148 pilus, toxins, ethanolamine utilization, and hemolysin; all of which having been associated with virulence and
149 pathogenesis [29]–[32].

150 We investigated the gene products and predicted genome-encoded pathogenic traits in common
151 within each clade, i.e., shared by all 5 strains tested per clade. A comparison between gene products, which
152 consider the whole genome (Supplementary Table 3), and the predicted genome-encoded pathogenic
153 properties (Supplementary Table 2), shows that the three clades share a higher percentage of predicted
154 pathogenic traits (47.36%) than gene products (14.23%; Extended Data Fig. 1a). Also of note is the high
155 percentage of gene products that are not shared by the tested strains of the three clades (>75%), when
156 compared to the lower percentage of predicted pathogenic traits that are not shared by all members of the
157 tested clades (<20%).

158 To assess the presence of gene products that might have clinical relevance, but not be included in
159 the available pathogenic properties databases, we analyzed the genomes of each strain for the number of
160 gene products related to the following categories: toxin-antitoxin, multidrug resistance, siderophores, LPS,
161 natural competence, conjugation, transposase, and phages/integrases. With this analysis, ARO112 shows
162 consistently lower number of gene products within these categories, and no gene product related to
163 conjugation or conjugal proteins, which are important for bacteria to acquire antibiotic resistance genes
164 (Extended Data Fig. 1b). Moreover, even though the genome analysis displays Kgr as the closest tested
165 relative to ARO112 (Fig. 1a) and the predicted pathogenic traits analysis hints at Kmi as closely related to
166 ARO112 (Fig. 1b), both Kgr and Kmi clearly differ from ARO112 when focusing on gene products for such
167 clinically-relevant categories (Extended Data Fig. 1b), indicating that ARO112 might be a different species
168 altogether.

169 Upon adding data for the abundance of each pathogenic property (Supplementary Table 4), instead
170 of the binary analysis of presence/absence (Fig. 1c), the strains were no longer segregated by taxonomy, and
171 instead segregated in two clusters along PCo 2 (Fig. 1d). One cluster included a known multi-drug resistant
172 (MDR) *K. pneumoniae* strain (MH258) and three strains isolated from hospitalized patients. The top 10
173 pathogenic traits driving the separation of the two clusters include several antimicrobial resistance-
174 associated properties (6/10; Supplementary Table 5), and accordingly these properties were enriched in the
175 cluster including the MDR *K. pneumoniae* strain. ARO112 was in the second cluster together with MBC022,
176 both isolated from non-antibiotic-treated gut microbiomes [24], and together with known non-MDR strains
177 like MG1655 (Fig. 1d). These results show that the predicted pathogenic properties encoded by the different
178 bacteria correlate with the taxonomy. However, the abundance of these properties segregates by the drug
179 resistance-encoded genes of individual isolates, regardless of taxonomy. ARO112 separated from known

180 MDR strain MH258 and clinical isolates Kp1012, Kp834, and Ec1898, and showed overall less predicted
181 pathogenic properties than the ensemble of other tested strains.

182

183 **ARO112 shows fewer traits associated with nosocomial infections**

184 Given that genome predictions do not always directly translate into phenotypes, we decided to
185 perform several in vitro tests for traits that are generally associated with *Enterobacteriaceae* pathogenicity
186 in nosocomial infections and gut colonization (Fig. 2a). For that, we selected a subset of the aforementioned
187 strains, including four *E. coli* strains (non-pathogenic K-12 MG1655 strain, pathobiont AIEC, probiotic EcN,
188 and clinical isolate Ec1898), three *K. pneumoniae* strains (clinical isolates MH258, Kp1012, and Kp834), and
189 two non-*pneumoniae Klebsiella* strains from our strain collection (MBC022, ARO112). We performed these
190 tests under two different laboratory conditions (nutrient rich – LB – and nutrient poor media – M9 salts
191 minimal medium with glucose) to evaluate if these pathogenic traits vary in different environments.

192 We started by testing antibiotic resistance, as this is the main driver of clinical problems associated
193 with *Enterobacteriaceae* [33], due to their efficient ability to acquire and share antibiotic resistance genes
194 from other bacteria through mechanisms like horizontal gene transfer (HGT) [34]. Our results showed that
195 ARO112, similar to MG1655, EcN, and MBC022, is not MDR since it displays resistance to less than three
196 classes of antibiotics (Fig. 2b). The other five strains tested showed resistance to three or less (AIEC),
197 depending on the medium, or more than three (Ec1898, Kp1012, Kp834, MH258) classes of antibiotics,
198 including, as expected, the known MDR strain MH258 in addition to the clinical isolates from hospitalized
199 patients Ec1898, Kp1012, and Kp834 (Fig. 2b), confirming their MDR status (Fig. 1d). Most of all, these results
200 confirm that ARO112 is not MDR and highlight that bacterial phenotypes are context dependent, with
201 minimal medium, frequently, potentiating resistance phenotypes.

202 Biofilms are microbial communities enclosed in extracellular matrix and adherent to a substrate and
203 can contribute to increased recalcitrance to antibiotic treatments [35]. We found that Kp1012 was the strain
204 that produced the most robust biofilm biomass, in minimal medium. In rich medium, most strains resulted in
205 low (EcN, Kp834, MBC022, ARO112) or very low (Ec1898, MH258) biofilm biomass (Fig. 2c), with only
206 MG1655, AIEC, and Kp1012 showing slightly higher biofilm biomass (Fig. 2c). Under minimal medium,
207 ARO112, Kp834, and MBC022 presented some capacity for biofilm formation, but much lower than Kp1012.
208 All *E. coli* strains and MH258 showed lower biofilm biomass (Fig. 2c).

209 Urease production is a common trait in *K. pneumonia* and *K. oxytoca* and can be problematic in
210 urinary tract infections, but might also be a good competitive trait for gut colonization [36]. In cultures grown
211 in rich medium there was no detectable urease activity, except for *K. oxytoca* MBC022 and, to a lesser extent,
212 ARO112, both displaying low levels of urease (Fig. 2d). In cultures grown in minimal medium all *Klebsiella*

213 strains, but not *E. coli* strains, showed significantly higher urease activity, with Kp1012 and MBC022
214 presenting the highest and Kp834, MH258, and ARO112 the lowest activities, with the latter with similar
215 levels to rich medium (Fig. 2d). The absence of urease activity in the *E. coli* strains is expected, since this
216 species is a known non-urease producer, albeit some clinical isolates of the pathogenic Enterohemorrhagic
217 *E. coli* have been shown to have urease activity [37]. Strains proficient in both biofilm formation and urease
218 production, as is the case for Kp1012, can become problematic and often associated with recurrent urinary
219 tract infections [38].

220 In rich medium, which is not limited in iron, all strains showed a reduced production of iron chelators,
221 siderophores (Fig. 2e). Interestingly, in iron-limited conditions, siderophore production was not increased in
222 ARO112, MG1655, nor MBC022, as opposed to the rest of the strains, where a significantly higher
223 siderophore production was observed (Fig. 2e).

224 When testing resistance to serum-mediated killing of bacteria grown in rich medium, only the *K.*
225 *pneumoniae* strains and MBC022 showed significant resistance to and replication ability in the presence of
226 human serum (Fig. 2f), indicating their potential capacity to survive and thrive in the bloodstream of patients.
227 On the contrary, most *E. coli* strains (MG1655, AIEC, EcN) are very susceptible to human serum, while Ec1898
228 and ARO112 are not killed by nor do they replicate in human serum (Fig. 2f). Interestingly, testing these
229 strains grown in minimal medium resulted in a significantly higher replication for MH258, increasing from 40-
230 (in rich medium) to 140-fold. More surprising, however, was the change observed for EcN; according to what
231 has been reported, EcN shows strong susceptibility to human serum [39] when grown in rich medium, but a
232 strong resistance and replication capacity when grown in minimal medium (70-fold increase; Fig. 2f). Reports
233 on this phenotype are usually performed using rich media to grow bacteria [40], but here we found that some
234 bacteria, like EcN and MH258, show increased proliferation when grown in minimal medium. Finally, ARO112
235 shows no evidence of being killed by the human serum, nor does it replicate to the levels seen for most
236 strains (Fig. 2f). Since this virulence trait directly affects the host, as it potentially allows bacteria to proliferate
237 in the bloodstream, with life-threatening risks, ARO112 inability to proliferate is a desirable trait for a
238 potential probiotic.

239 The evaluation of the pathogenic potential based on phenotypic assays gives us the resolution to the
240 strain level regarding this selection of virulence traits. While the genome-based approach showed us that the
241 virulence traits predicted to be present or absent in the genome correlate to the taxonomy, the selective
242 testing of clinically-important phenotypes allows us to distinguish distinctly active virulence traits within a
243 taxon, such as the heterogeneity within both the *E. coli* and the *K. pneumoniae* clades, but also to pinpoint
244 strains with overall less pathogenic traits associated with nosocomial infections. Of note, ARO112 stands out
245 with low pathogenic traits commonly associated with nosocomial infections.

246

247 **ARO112 is resistant to acquisition and efficient in curing plasmids bearing antibiotic resistance**

248 The lack of resistance found in the commensal non-clinical strains does not exclude the potential for
249 antibiotic resistance acquisition by HGT, which is common among *Enterobacteriaceae* within complex
250 communities, like the gut microbiota [41]. Indeed, the acquisition of antibiotic resistance, in particular by
251 HGT events, has been shown to be problematic, with *Enterobacteriaceae* at the forefront of this increasingly
252 concerning medical issue [34]. Therefore, we assessed the capacity of ARO112 to acquire resistance from
253 donor bacteria through HGT, in comparison with the probiotic EcN and the MDR *K. pneumoniae* strain that
254 had typical phenotypes of causative agents of nosocomial infections, Kp1012. We tested the transfer of a
255 commonly used conjugative plasmid (RP4) from a donor strain (MG1655 or Kgr) into the aforementioned
256 recipient strains. Interestingly, the already MDR strain Kp1012 had the highest acquisition rate, with a median
257 of 83% and 25% of cells acquiring the plasmid from the MG1655 and Kgr donors, respectively (Fig. 2g). EcN
258 presented an intermediate transfer rate, with a median of 25% and 4% acquiring the plasmid and consequent
259 antibiotic resistance from MG1655 and Kgr, respectively (Fig. 2g). In contrast, ARO112 showed a strong
260 resistance to plasmid acquisition, with a median of less than 4% of the population acquiring the RP4 plasmid
261 from MG1655 donor strain, and less than 0.5% from Kgr donor strain (Fig. 2g). Next, we tested the capacity
262 to retain the acquired plasmids, after five days of daily passages in rich or minimal media in the absence of
263 antibiotic selection. Remarkably, ARO112 showed the highest plasmid loss, with 87% and 65% of the
264 population losing the plasmid in rich and minimal media, respectively (Fig. 2h). In contrast, the MDR strain
265 Kp1012 lost the plasmid in 27% and 2% of the population, in rich and minimal media, respectively, and EcN
266 lost the plasmid in 61% and 34% of the population in rich and minimal media, respectively (Fig. 2h).

267 Even plasmids that are non-self-transmissible, can be transferred among bacteria, through
268 conjugation events [42] in which non-conjugative plasmids take advantage of conjugative plasmids'
269 machinery from the donor strain. We have also tested the capacity of ARO112, EcN, and Kp1012 to retain a
270 non-conjugative plasmid (pMP7605) carrying an antibiotic resistance received by electroporation. Kp1012
271 barely lost the plasmid, both in rich (7%) and minimal media (11%; Fig. 2i), and 42% of EcN colonies lost the
272 non-conjugative plasmid in rich medium (Fig. 2i), while no loss was observed in minimal medium (Fig. 2i).
273 Remarkably, ARO112 showed the highest plasmid loss, with 83% and 51% of the population losing the non-
274 conjugative plasmid when grown in rich or minimal media, respectively (Fig. 2i).

275 Natural plasmids are known to be more stably maintained as they often confer some fitness
276 advantages that drive their persistence [43]. We also tested the retention capacity of a Kanamycin resistance-
277 bearing natural plasmid(s) transferred from one of the MDR clinical isolates, Kp834, into ARO112 and EcN
278 (Kp1012 was not tested due to its MDR complicating counterselection). EcN did not lose the plasmid, while

279 ARO112 lost the plasmid in over 15% (rich medium) and 30% (minimal medium) of the population (Extended
280 Data Fig. 2b).

281 In summary, even though ARO112 shares with other *Enterobacteriaceae* strains the capacity to
282 acquire plasmids, when compared to the probiotic strain EcN and the *K. pneumoniae* clinical isolate Kp1012,
283 ARO112 displays a significantly lower efficiency in plasmid acquisition and retention, a main source of
284 antimicrobial resistance in *Enterobacteriaceae* and, therefore, presents a reduced risk of becoming a clinical
285 problem.

286 **Bacterial pathogenic phenotypes can be altered upon gut colonization**

287 Having observed that the tested phenotypes varied depending on the culture medium used, we
288 questioned which of the tested laboratory media, rich or minimal, was resembling the phenotypical profiles
289 of bacteria in the mammalian gut more closely. Therefore, we tested the phenotypes whose assays do not
290 require bacterial growth, in bacteria collected directly from fecal samples from mono-colonized mice (Fig.
291 3a). We compared the phenotypes in ARO112 with EcN and Kp1012 collected from fecal samples of ex-germ-
292 free mice colonized for five days with each of these bacteria, without selection or growth. Regarding urease
293 activity, Kp1012 presented the same high urease activity detected in minimal medium-grown cultures and
294 EcN showed the expected low urease activity also observed in all laboratory-grown cultures (Fig. 3b and 2d),
295 ARO112 presents a variable phenotype, with half the samples showing low urease activity, similar to the
296 results obtained with cultures grown in the laboratory, while the other half showed increased urease activity
297 (Fig. 3b and 2d). This result, while surprising due to the low levels of urease activity in culture-grown ARO112,
298 indicates that in this bacterium this phenotype is regulated differently in the gut environment. Interestingly,
299 fecal siderophore measurements showed low values for all three strains, but with a similar tendency
300 observed in minimal medium of lower values for ARO112, when compared with both EcN and Kp1012
301 (Extended Data Fig. 3a and Fig. 2e).

302 When testing for resistance to human serum after gut colonization, similar results were obtained
303 with bacteria extracted directly from feces of mono-colonized mice (Fig. 3c) to the ones of laboratory-grown
304 cultures (Fig. 2f). When compared to both Kp1012 and EcN, ARO112 strain is more sensitive human serum,
305 even when grown in mice (Fig. 3c), therefore being a safer strain for clinical settings than the probiotic EcN.

306 We also checked the non-conjugative plasmid retention in the murine gut by having each strain
307 colonizing germ-free mice carrying the non-conjugative plasmid pMP7605, and quantifying how much of the
308 population retained the plasmid after five days of colonization. EcN lost the plasmid in only 11% of the
309 population, while Kp1012 lost in 51% (Fig. 3d). Remarkably, ARO112 lost the plasmid in more than 99% of
310 cells (Fig. 3d), showing that the recalcitrance of ARO112 to maintaining acquired antibiotic resistance is
311 potentiated in the murine gut.

312 Next, we tested the host reaction to the colonization by each of the three aforementioned strains,
313 by assessing the fecal levels of Lipocalin-2 (Lcn2), as a marker for gut inflammation [44], [45]. After 5 days of
314 mono-colonization, fecal levels of Lcn2 in mice colonized with ARO112 were similar to germ-free mice,
315 providing no evidence for ARO112 inducing intestinal inflammation in mono-colonized animals (Fig. 3e). This
316 contrasted with colonization with EcN and, to an even greater extent, with Kp1012, which significantly
317 induced Lcn2 when compared to the germ-free mice levels (Fig. 3e). Since Lcn2 decreases bacterial growth
318 through siderophore sequestration, we then decided to test how these three strains were able to maintain
319 growth with increasing levels of Lcn2, which is commonly increased in the inflamed intestinal environment.
320 ARO112, EcN, or Kp1012 were grown in rich or minimal media in the absence or in the presence of increasing
321 concentrations of Lcn2. ARO112 showed an overall higher resistance than EcN to increased levels of Lcn2
322 (Extended Data Fig. 3b), suggesting a better ability to survive in an inflamed gut environment.

323 Together, these results indicate that ARO112 could be an optimum next-generation probiotic since
324 it has reduced resistance to human serum and low plasmid retention and low pathogenic potential.
325 Moreover, it has low plasmid retention, as opposed to other *Enterobacteriaceae* strains. Additionally,
326 ARO112's ability to endure high levels of Lcn2 with no inflammatory induction, as opposed to EcN, further
327 highlights how this commensal strain is potentially safer and better suited to compete with invading bacteria
328 in intestinal inflammatory environments.

329

330 **ARO112 promotes a faster recovery from AIEC infection in an IBD mouse model**

331 Having shown that ARO112 has less potentially harmful features than an MDR *K. pneumoniae* and
332 the probiotic EcN and that in previous work we also see that ARO112 is able to partially displace *E. coli*
333 MG1655 from the gut of in mono-colonized and antibiotic-treated mice [24], here, we decided to test the
334 potential protective role of ARO112 against AIEC. The pathobiont AIEC is particularly problematic under
335 inflammatory conditions, such as those in IBD patients. Therefore, we reasoned that the low inflammatory
336 potential of ARO112 and its capacity to endure Lcn2 could be beneficial in the IBD context.

337 It was previously shown that a genetic-based murine model for IBD, Nod2$^{-/-}$ mutant mice, is more
338 susceptible to AIEC colonization after antibiotic treatment, similar to IBD patients, as clearance of this
339 pathobiont is slower in the Nod2$^{-/-}$ animals than in WT animals [46]. Additionally, like IBD patients, Nod2$^{-/-}$
340 animals are more prone to gut inflammation increases [47], [48]. Therefore, we started by comparing
341 susceptibility of WT and Nod2$^{-/-}$ mice to colonization by AIEC in our animal facility. All mice were treated by
342 oral gavage with a combination of two non-absorbed antibiotics used in clinical settings on IBD patients [49],
343 vancomycin and gentamicin, once daily for three consecutive days [46] (Fig. 4 and Extended Data Fig. 4a).
344 After antibiotic treatment, mice were gavaged with AIEC, and AIEC colonization was followed through

345 selective plating. As observed by others [46], Nod2$^{-/-}$ mice were more susceptible to AIEC colonization in
346 comparison with WT mice, with ~50% of the Nod2$^{-/-}$ mice still being colonized with AIEC after 20 days of
347 infection (Fig. 4b, control mice), while all WT mice had cleared the infection in that timeframe (Extended
348 Data Fig. 4a, control mice). To test the therapeutic potential of ARO112, one day following AIEC infection,
349 Nod2$^{-/-}$ control mice (PBS) were compared with Nod2-/- mice gavaged with either ARO112 strain or the
350 probiotic EcN strain (Fig. 4a). AIEC decolonization was faster in mice treated with ARO112, with 50% of the
351 animals being AIEC-free at 8 days of infection (7 days of probiotic treatment), compared to mice that received
352 no probiotic treatment, in which 14 days were needed for 50% of the mice to resolve the infection, and 7 out
353 of 15 mice still remained infected at the end of treatment (Fig. 4b,c). Surprisingly, treatment with the
354 probiotic EcN did not help decolonization, but actually resulted in a worse outcome, with all but one tested
355 mouse remaining infected with high levels of AIEC for the 20 days of the experiment (Fig. 4b,c). We highlight
356 that the one mouse of this group that displaced AIEC infection, was never colonized with EcN and therefore,
357 the displacement observed in this animal is not attributed to the EcN treatment (Extended Data Fig. 4b).
358 When assessing the number of mice that resolve the infection in each condition, it is evident that treatment
359 with EcN promotes a continued infection with AIEC, while the absence of probiotic treatment led to the
360 infection being resolved in half of the population (Fig. 4b,c), thus the outcome obtained with the treatment
361 with ARO112, in which 10 out of 12 mice (>83%) became AIEC-free by the end of the experiment, was more
362 efficient than the control (Fig. 4b). Additionally, we observed that ARO112 is itself cleared from the intestinal
363 microbiota throughout the experiment after AIEC, with a median of 10 days post-AIEC inoculation for the
364 ARO112 loads to drop below detection level in 50% of mice (Extended Data Fig. 4b), having disappeared in 9
365 out of the 12 mice tested (75%) by the end of the experiment (Extended Data Fig. 4c). Interestingly, the
366 protective effect of ARO112 observed in Nod2$^{-/-}$ mice was not seen in WT mice treated with the same
367 antibiotic regimen, where AIEC decolonization was observed in all the animals independently of the
368 treatment (Extended Data Fig. 4a).

369 We have previously shown [24] that ARO112 could partially displace MG1655 in WT mice with a more
370 severe antibiotic treatment of two weeks of streptomycin in the drinking water, which drastically affects the
371 microbiota composition and facilitates *Enterobacteriaceae* colonization that compete for the available
372 carbon sources. We tested the effect of ARO112 and EcN on AIEC in streptomycin-treated WT mice where,
373 in contrast to what we had observed with MG1655, neither ARO112 nor EcN were able to displace AIEC
374 (Extended Data Fig. 4d). Moreover, in the absence of a microbiome in mice mono-colonized with AIEC, a
375 limited displacement of AIEC was obtained upon co-colonization with ARO112 (~4 fold; Extended Data Fig.
376 4e), which was similar to what was observed when co-colonized with other *Enterobacteriaceae* like the MDR
377 clinical isolates Ec1898 and Kp1012 (>4 and ~6, respectively; Extended Data Fig. 4f,h), but lower than the >10
378 fold seen previously against MG1655 [24] or against other Pseudomonadota species like *Vibrio cholerae* (>38;

379 Extended Data Fig. 4g). Interestingly, when co-cultured in vitro in minimal medium to test for competition
380 for carbon sources, ARO112 had minimal effect on AIEC growth as opposed to EcN that seemed to highly
381 reduce AIEC loads (Extended Data Fig. 4i). Together, these results show that ARO112 does not strongly
382 compete directly with AIEC in these environments and indicate that the mechanisms explaining the
383 displacement of AIEC in the Nod2$^{-/-}$ animals do not seem to rely on a direct ARO112 effect on AIEC
384 colonization and rather indicate the potential involvement of the gut microbiota. This contrasts from what
385 we showed before for MG1655, where we could demonstrate that the reduction in MG1655 colonization
386 mediated by ARO112, was largely mediated by the direct interaction between these 2 species through
387 nutrient competition as the ARO112-dependent inhibition of MG1655 could be observed with in vitro
388 cultures and in germ-free mono-colonized mice [24]. This highlights that ARO112 can have a broad range
389 effect on different Pseudomonadota pathogens, and most likely with different mechanisms to outcompete
390 other bacteria.

391

392 **ARO112 treatment promotes microbiota recovery, namely potential butyrate-producing bacteria depleted**
393 **by antibiotic treatment**

394 Whether ARO112 effect on AIEC in the IBD model is a result of the direct interplay with the host
395 genetic background, the gut microbiota, the inflammatory status, or all of the above, is not clear. However,
396 our results indicate that this outcome does not seem to rely on a direct ARO112 effect on AIEC growth.
397 Nonetheless, the fact that we observed that in highly damaged gut microbiotas due to severe antibiotic
398 regimens (14 days of streptomycin) or in the absence of a gut microbiota (ex-germ-free animals), ARO112's
399 effect on AIEC was greatly diminished, together with the fact that ARO112 itself was removed from the gut
400 after the AIEC displacement in the Nod2$^{-/-}$ mice, led us to evaluate a possible role of the gut microbiota in
401 this process. We analyzed the microbiota composition of Nod2$^{-/-}$ mice by 16s rRNA gene sequencing before
402 (pre-AB) and after (post-AB) antibiotic treatment, as well as post-AIEC colonization and after treatments with
403 PBS, EcN, or ARO112. We observed that mice treated with ARO112 showed a significant recovery in richness
404 and a tendency in recovery of diversity, unlike the long-lasting decrease of both metrics in the mice that
405 received no probiotic treatment or EcN, which persisted as low as with antibiotic treatment (Fig. 5a,b). This
406 microbiota recovery promoted by the treatment with ARO112 can help explain both the better displacement
407 of AIEC in this group, but also the displacement of ARO112 itself (Extended Data Fig. 4b,c), as we expect the
408 recovering microbiota to develop colonization resistance.

409 We then analyzed which of the most abundant taxa (37 taxa representing an average of 98%
410 abundance of all taxa) were affected by the antibiotic treatment. Out of these 37 taxa, 22 (59%) were
411 depleted by the antibiotics, while 7 (19%) were enriched and 8 (22%) remained unchanged during the

412 antibiotic treatment (Fig. 5c). The mice from the control group or treated with EcN were able to recover 14%
413 (3 of 22) taxa depleted by the antibiotic treatment (Fig. 5c). When treated with ARO112 strain, mice were
414 able to recover 41% (9 of 22) taxa depleted by the antibiotic treatment (Fig. 5c).

415 A deeper analysis of the groups of bacteria affected by antibiotic treatment showed that of the 8
416 taxa of potential butyrate producers depleted by the antibiotics, 4 recovered upon almost 20 days post-
417 treatment with ARO112 (*Dorea*, *Lachnospiraceae*, *Oscillibacter* and *Ruminococcaceae*), while only 1 was
418 recovered in the control (*Lachnospiraceae*) and another with EcN treatment (*Alistipes*) (Fig. 5c). Overall, we
419 can see a better and faster recovery of these 4 taxa upon treatment with ARO112, with 3 of them showing
420 significantly increased levels as early as 4 days post-treatment (day 5 post-infection with AIEC), one of which,
421 *Lachnospiraceae*, already recovered to pre-AB levels (Fig.5d). Animals that were not treated with ARO112
422 either show a delayed recovery or no recovery at all of these potential butyrate producers (Fig. 5d).

423 PCoA analysis shows that before antibiotic treatment (pre-AB) samples cluster tightly together,
424 whereas after (post-AB) samples were more dispersed (Extended Data Fig. 5a), revealing a stochastic effect
425 of the antibiotics. Treatment with PBS (Ctrl) increased the dispersion of the samples, with 29% (4/14) of
426 samples positioning close to pre-AB samples, 50% (7/14) remaining close to the post-AB samples, and 21%
427 (3/14) in neither proximity. Treatment with EcN resulted in 90% (9/10) of samples clustering tightly and away
428 from both pre- and post-AB samples, while 1 sample was positioned with the pre-AB samples (this was the
429 aforementioned mouse that was resisted colonization by EcN). Interestingly, treatment with ARO112
430 probiotic showed 40% (4/10) of samples placed close to the pre-AB samples, while 50% (5/10) remained in
431 close to post-AB samples, and only 1 sample occupying a region apart from both pre- and post-AB samples
432 (Extended Data Fig. 5a). Plotting only the 4 taxa of putative butyrate producers that are depleted by
433 antibiotics and recover after treatment (*Dorea*, *Oscillibacter*, *Lachnospiraceae*, and *Ruminococcaceae*), we
434 noticed that, unlike the treatment with EcN, the microbiota composition treated with PBS or ARO112
435 probiotic cluster closely with pre-AB samples (Extended Data Fig. 5b).

436 IBD patients experience blooms of Pseudomonadota, in particular after antibiotic treatment, a
437 reason of concern due to the several members of this phylum that present pathogenic potential. Accordingly,
438 we also observed 3 taxa of Pseudomonadota, *Escherichia*/*Shigella*, *Enterobacteriaceae*, and *Proteus,* that are
439 usually considered pathobionts, that bloomed after antibiotics. This bloom was transient in the control group
440 and the group treated with ARO112, but not with EcN treatment (Fig. 5c; Extended Data Fig. 5d).

441 In summary, here we show how in a mouse model susceptible to infection and prone to
442 inflammation, ARO112 targeted several of the microbiota-based IBD hallmarks, by displacing the invading
443 pathobiont AIEC, while promoting recovery of the dysbiotic microbiota, by reducing Pseudomonadota and
444 increasing potential butyrate producers.

445

446 **Probiotic therapy with ARO112 enhances microbiota production of butyrate and prevents intestinal**
447 **inflammation**

448 As described in the above section, treatment with ARO112 leads to a better recovery of microbiota
449 richness and diversity, including potential butyrate-producing bacteria. Studies have tagged short-chain fatty
450 acids (SCFAs) like butyrate, acetate, and propionate as important metabolites in IBD, with depletion of
451 butyrate-producing gut bacteria by antibiotic treatments being considered a clinical outcome in these
452 patients [14], [50]. Moreover, oral administration of butyrate to improve IBD outcomes in patients has been
453 proposed [51]. Therefore, our observation that ARO112 treatment promotes potential butyrate producers in
454 the microbiota, possibly leading to an increased and sustained production of butyrate within the microbiota
455 and gut epithelium, instead of the need for continuous exogenous administration, could be very relevant.
456 For that reason, we have assessed SCFA concentrations in fecal samples of mice treated with probiotics or
457 untreated (Fig. 6a). In agreement with our previous results showing the increase of potential butyrate-
458 producing bacteria, treatment with ARO112 resulted in a clear increase of fecal levels of butyrate when
459 compared to mice treated with PBS or with EcN (Fig. 6a). An increase in isobutyrate (an isomer of butyrate)
460 and acetate was also observed with the ARO112 treatment in comparison with the control group and EcN-
461 treated mice, although not statistically significant. Propionate levels were significantly higher with ARO112
462 than with PBS, but similar to the levels in EcN group. On the other hand, succinate showed higher, but not
463 significantly, values in mice treated with EcN, when compared to mice treated with PBS or ARO112 probiotic
464 (Fig. 6a).

465 Butyrate has been linked to healthy gut states, with anti-inflammatory properties [52], while
466 succinate has been touted as an inflammation marker [53]. Therefore, we used Lcn2 to evaluate the intestinal
467 inflammatory response of the Nod2$^{-/-}$ mice infected with AIEC and treated with PBS, ARO112, or EcN.
468 Interestingly, treatment with EcN not only led to persistent infection by AIEC but also resulted persistently
469 high Lcn2 levels (Fig. 6b), unlike PBS treatment, in which Lcn2 levels varied between animals, having a
470 significant but transient increase at day 5 of infection (Fig. 6b). More importantly, mice treated with ARO112
471 showed persistently low levels of Lcn2, never significantly varying from the levels prior to antibiotic treatment
472 (Fig. 6b).

473 When assessing metrics for infection and recovery, such as microbiota diversity and richness,
474 infection duration, intestinal inflammation, and intestinal butyrate levels, we have noticed that in the control
475 group there is a significant negative correlation between infection duration and both diversity and richness,
476 supporting a link between microbiota recovery and clearance of infection (Supplementary Table 7). On the
477 other hand, mice treated with ARO112 do not show that significant correlation, demonstrating that the

478 infection clearance is not solely linked to microbiota recovery, with other therapeutic effects in play
479 (Supplementary Table 7).

480 The reduced Lcn2 levels observed upon treatment with ARO112 is befitting the previous data
481 showing increased butyrate in the gut, since a link between this SCFA and low inflammatory states has been
482 made before [52]. Similarly, the higher levels of succinate present in mice treated with EcN are also in
483 agreement with their higher Lcn2 levels. However, because the preventive effect on inflammation promoted
484 by ARO112 treatment was seen as early as 5 days post-infection, we can speculate that the recovery of
485 *Lachnospiraceae* seen with ARO112 by day 5 might be responsible for the anti-inflammatory effect of
486 butyrate at this timepoint. These results indicate that ARO112 treatment leads to a prevention of
487 inflammation, which in turn can also promote recovery of the microbiota, including butyrate producers,
488 whose increased production of butyrate might further contribute to the anti-inflammatory intestinal
489 environment and further recovery of the microbiota from pathobiont expansion and dysbiosis. Moreover,
490 the possible pro-inflammatory potential of EcN also highlights ARO112 as a safer probiotic in both non-
491 inflammatory or inflammatory host states.

492 The ensemble of these results, namely the displacement of AIEC, the prevention of inflammation,
493 and the recovery of the dysbiotic microbiota and butyrate, all obtained upon treatment with ARO112, show
494 a three-pronged therapy targeting the three hallmarks of IBD.

495

496 **Discussion**

497 The main characteristic of a healthy intestinal microbiome is its richness and diversity of microbes
498 and metabolites that sustain its protective role. Its robustness, however, is greatly affected by extrinsic
499 factors, such as medical treatments and changing diets. Our understanding of the functional aspects driving
500 this protection by a balanced microbiota is still limited. The importance of identifying protecting bacteria to
501 be used as therapeutics is unprecedented and research has been driven by the discovery and characterization
502 of the beneficial effects those bacteria can provide.

503 Here, we showed that our previously identified microbiota member of the non-*pneumoniae*
504 *Klebsiella* complex, *Klebsiella* sp. ARO112 strain [24], is able to displace the pathobiont AIEC from an IBD
505 mouse model, while preventing inflammatory flares and mediating the recovery of an imbalanced
506 microbiota. The therapeutic effect of ARO112 is multifactorial, affecting all three main hallmarks of intestinal
507 inflammatory disorders: gut inflammation, dysbiosis, and susceptibility to infection. Our results show that in
508 the presence of ARO112 there is a faster recovery of microbiota members producers of butyrate which is
509 reflected in an increase in intestinal butyrate levels, a SCFA known to be important for gut health, including
510 in mediating clearance of MDR *Enterobacteriaceae* by direct inhibition [54]. Other studies have shown that

511 some members of the microbiota (belonging to *Lactobacillus* genus) can contribute to promote clearance of
512 MDR *K. pneumoniae* by driving the recovery of *Clostridiales* [55]. Similarly, a study focusing on human
513 samples showing colonization resistance against intestinal pathogens with high risk of bacteremia found an
514 enrichment of non-*pneumoniae Klebsiella* species, whose protective effect was then validated in murine
515 models [27]. A previous study had already pinpointed, and validated, *K. oxytoca* strains present in children's
516 microbiota with protection against invading *K. pneumoniae* [26], in the aftermath of our previous publication
517 showing ARO112 as protective against *E. coli* and *Salmonella* Typhimurium [24]. These three studies
518 highlighting the protective role of non-*pneumoniae Klebsiella* species against *Enterobacteriaceae* invasion,
519 display the important role of nutrient competition in this interaction. Nevertheless, all these studies are
520 focused on colonization resistance and pathogen displacement. Here, we show that ARO112 therapeutic
521 effect goes beyond nutrition competition, even being able to clear a clinically-important pathobiont, AIEC, in
522 a disease model for intestinal inflammation, not relying on this direct competition effect, with an astounding
523 >83% success rate. Our results, however, are not solely focused on the important and decisive pathogen
524 clearance, but also showing that ARO112 probiotic treatment engages the native butyrate producers
525 depleted by antibiotic treatment into microbiota recovery and prevent inflammatory episodes in the process.

526 Even though some protective capabilities seem to be shared by different non-*pneumoniae Klebsiella*
527 species, when considering bacteria as potential probiotics, their pathogenic potential and safety also need
528 to be considered. Our pipeline for strains' characterization shows that their pathogenic potential can be
529 context-dependent, emphasizing how important it is to test different conditions before asserting the
530 virulence status of a potential probiotic. We show how ARO112 presents a reduced pathogenic potential and
531 is safer than other potential protective bacteria, such as *K. oxytoca* or *E. coli* Nissle 1917, both by displaying
532 less pathogenic phenotypes, but also by being more recalcitrant to antibiotic resistance acquisition and
533 maintenance compared to *E. coli* Nissle 1917, therefore not contributing to the currently increasing antibiotic
534 resistance pandemic.

535 Having a safe protective microbiota member that can be used to promote a faster recovery of an
536 imbalanced microbiota and displace pathogens or pathobionts, while preventing inflammatory flares in
537 disease context is of great therapeutic importance, and a major leap in current probiotic research knowledge
538 and capabilities. Further research is needed to deepen the understanding of the mechanisms driving ARO112
539 protection, which will open up new avenues for the identification and characterization of more microbiota
540 members and consortia with safe therapeutic potential for clinical use, which can then be engineered to
541 tackle a myriad of clinically relevant disorders.

542

543

Acknowledgements

We thank the members of the Bacterial Signalling Laboratory at Instituto Gulbenkian Ciência and Tanja Dapa, and João Xavier for critically reading the manuscript. In particular, we thank Joana Amaro for the help processing samples for genomic sequencing and metabolomics. We also thank Instituto Gulbenkian Ciência's Animal Facility, in particular Joana Bom, and the Genomics Facility, namely João Sobral, for the help provided during this project's execution. The authors would like to thank the Microbiology Service from the Hospital La Fé in Valência (Spain) for isolating and providing the strains Ec1898, Kp834, and Kp1012. I would like to thank Gabriel Nuñez for providing the AIEC strain (LF82), and Roberto Balbontín-Soria for providing the plasmid pMP7605. We would also like to acknowledge Nassos Typas for the suggestion to test conjugation from a clinical isolate.

This work was funded by Fundação para a Ciência e Tecnologia (FCT) projects [PTDC/BIA-MIC/6990/2020] and [SFRH/BPD/116806/2016], as well as by Municipality of Oeiras Proof-of-Concept InnOValley 2022 [IOVPoC-2022-21] and a European Commission grant [MSCA-IF-2018-843183]. Additionally, this project was also funded by InfectERA-ERANET- through FCT grant (InfectERA/0004/2015) and *Acciones complementarias* grant [PCIN-2015-094] from the Spanish Ministerio de Economía y Competitividad and the 7th Research framework program from EU, and a grant from the Spanish MICINN [PID2020-120292RB-I00], granted to KBX and CU, respectively.

Author contributions

V.C. and R.A.O conceptualized and designed the research studies. M.B.C. performed in vivo experiments with *V. cholerae* and *Ec1898*, under the supervision of R.A.O. and K.B.X.. M.F.P. performed the NMR under the supervision of K.B.X.. R.A.O. executed in vitro experiments with support from V.C.. V.C. executed in vivo experiments with AIEC and Kp1012, in SPF wildtype, SPF Nod2$^{-/-}$, and GF wildtype models, with support from R.A.O.. R.A.O. analyzed sequencing data. V.C., and R.A.O. analyzed and interpreted all the data, under the supervision of K.B.X.. V.C. and R.A.O. wrote the first draft of the manuscript with valuable input from K.B.X. All authors critically read and approved the manuscript.

Competing interests

A provisional patent application has been filed by the Gulbenkian Foundation based on this work.

575 **References**

576 [1] P. J. Turnbaugh, M. Hamady, T. Yatsunenko, B. L. Cantarel, A. Duncan, R. E. Ley, M. L. Sogin, W. J.
577 Jones, B. A. Roe, J. P. Affourtit, M. Egholm, B. Henrissat, A. C. Heath, R. Knight, and J. I. Gordon, "A
578 core gut microbiome in obese and lean twins.," *Nature*, vol. 457, no. 7228, pp. 480–484, Jan. 2009,
579 doi: 10.1038/nature07540.

580 [2] E. B. Hollister, C. Gao, and J. Versalovic, "Compositional and functional features of the
581 gastrointestinal microbiome and their effects on human health.," *Gastroenterology*, vol. 146, no. 6,
582 pp. 1449–1458, May 2014, doi: 10.1053/j.gastro.2014.01.052.

583 [3] R. A. Oliveira, V. Cabral, and K. B. Xavier, "Microbiome–diet interactions drive antibiotic efficacy,"
584 *Nat. Microbiol.*, vol. 6, no. 7, pp. 824–825, 2021, doi: 10.1038/s41564-021-00926-8.

585 [4] A. Andremont, J. Cervesi, P.-A. Bandinelli, F. Vitry, and J. de Gunzburg, "Spare and repair the gut
586 microbiota from antibiotic-induced dysbiosis: state-of-the-art," *Drug Discov. Today*, vol. 26, no. 9,
587 pp. 2159–2163, 2021, doi: https://doi.org/10.1016/j.drudis.2021.02.022.

588 [5] R. A. Oliveira and E. G. Pamer, "Assembling symbiotic bacterial species into live therapeutic
589 consortia that reconstitute microbiome functions.," *Cell Host Microbe*, vol. 31, no. 4, pp. 472–484,
590 Apr. 2023, doi: 10.1016/j.chom.2023.03.002.

591 [6] N. Jain, T. P. Umar, A.-F. Fahner, and V. Gibietis, "Advancing therapeutics for recurrent clostridioides
592 difficile infections: an overview of vowst's FDA approval and implications.," *Gut Microbes*, vol. 15,
593 no. 1, p. 2232137, 2023, doi: 10.1080/19490976.2023.2232137.

594 [7] Z. DeFilipp, P. P. Bloom, M. Torres Soto, M. K. Mansour, M. R. A. Sater, M. H. Huntley, S. Turbett, R.
595 T. Chung, Y.-B. Chen, and E. L. Hohmann, "Drug-Resistant E. coli Bacteremia Transmitted by Fecal
596 Microbiota Transplant.," *N. Engl. J. Med.*, vol. 381, no. 21, pp. 2043–2050, Nov. 2019, doi:
597 10.1056/NEJMoa1910437.

598 [8] S. Gupta, B. H. Mullish, and J. R. Allegretti, "Fecal Microbiota Transplantation: The Evolving Risk
599 Landscape.," *Am. J. Gastroenterol.*, vol. 116, no. 4, pp. 647–656, Apr. 2021, doi:
600 10.14309/ajg.0000000000001075.

601 [9] A. Goethel, K. Croitoru, and D. J. Philpott, "The interplay between microbes and the immune
602 response in inflammatory bowel disease.," *J. Physiol.*, vol. 596, no. 17, pp. 3869–3882, Sep. 2018,
603 doi: 10.1113/JP275396.

604 [10] P. Qiu, T. Ishimoto, L. Fu, J. Zhang, Z. Zhang, and Y. Liu, "The Gut Microbiota in Inflammatory Bowel
605 Disease.," *Front. Cell. Infect. Microbiol.*, vol. 12, p. 733992, 2022, doi: 10.3389/fcimb.2022.733992.

606 [11] M. Fakhoury, R. Negrulj, A. Mooranian, and H. Al-Salami, “Inflammatory bowel disease: clinical
607 aspects and treatments.,” *J. Inflamm. Res.*, vol. 7, pp. 113–120, 2014, doi: 10.2147/JIR.S65979.

608 [12] P. M. Irving, S. de Lusignan, D. Tang, M. Nijher, and K. Barrett, “Risk of common infections in people
609 with inflammatory bowel disease in primary care: a population-based cohort study.,” *BMJ open*
610 *Gastroenterol.*, vol. 8, no. 1, Feb. 2021, doi: 10.1136/bmjgast-2020-000573.

611 [13] A. B. Pithadia and S. Jain, “Treatment of inflammatory bowel disease (IBD).,” *Pharmacol. Rep.*, vol.
612 63, no. 3, pp. 629–642, 2011, doi: 10.1016/s1734-1140(11)70575-8.

613 [14] P. T. Santana, S. L. B. Rosas, B. E. Ribeiro, Y. Marinho, and H. S. P. de Souza, “Dysbiosis in
614 Inflammatory Bowel Disease: Pathogenic Role and Potential Therapeutic Targets.,” *Int. J. Mol. Sci.*,
615 vol. 23, no. 7, Mar. 2022, doi: 10.3390/ijms23073464.

616 [15] C.-L. N. Small, S. A. Reid-Yu, J. B. McPhee, and B. K. Coombes, “Persistent infection with Crohn’s
617 disease-associated adherent-invasive Escherichia coli leads to chronic inflammation and intestinal
618 fibrosis.,” *Nat. Commun.*, vol. 4, p. 1957, 2013, doi: 10.1038/ncomms2957.

619 [16] B. P. Abraham and E. M. M. Quigley, “Probiotics in Inflammatory Bowel Disease.,” *Gastroenterol.*
620 *Clin. North Am.*, vol. 46, no. 4, pp. 769–782, Dec. 2017, doi: 10.1016/j.gtc.2017.08.003.

621 [17] M. Schultz, “Clinical use of E. coli Nissle 1917 in inflammatory bowel disease.,” *Inflamm. Bowel Dis.*,
622 vol. 14, no. 7, pp. 1012–1018, Jul. 2008, doi: 10.1002/ibd.20377.

623 [18] H. Matthes, T. Krummenerl, M. Giensch, C. Wolff, and J. Schulze, “Clinical trial: probiotic treatment
624 of acute distal ulcerative colitis with rectally administered Escherichia coli Nissle 1917 (EcN).,” *BMC*
625 *Complement. Altern. Med.*, vol. 10, p. 13, Apr. 2010, doi: 10.1186/1472-6882-10-13.

626 [19] S. C. Bischoff, P. Bager, J. Escher, A. Forbes, X. Hébuterne, C. L. Hvas, F. Joly, S. Klek, Z. Krznaric, J.
627 Ockenga, S. Schneider, R. Shamir, K. Stardelova, D. V. Bender, N. Wierdsma, and A. Weimann,
628 “ESPEN guideline on Clinical Nutrition in inflammatory bowel disease,” *Clin. Nutr.*, vol. 42, no. 3, pp.
629 352–379, 2023, doi: https://doi.org/10.1016/j.clnu.2022.12.004.

630 [20] J. Suez, N. Zmora, G. Zilberman-Schapira, U. Mor, M. Dori-Bachash, S. Bashiardes, M. Zur, D. Regev-
631 Lehavi, R. Ben-Zeev Brik, S. Federici, M. Horn, Y. Cohen, A. E. Moor, D. Zeevi, T. Korem, E. Kotler, A.
632 Harmelin, S. Itzkovitz, N. Maharshak, *et al.*, “Post-Antibiotic Gut Mucosal Microbiome Reconstitution
633 Is Impaired by Probiotics and Improved by Autologous FMT.,” *Cell*, vol. 174, no. 6, pp. 1406-
634 1423.e16, Sep. 2018, doi: 10.1016/j.cell.2018.08.047.

635 [21] E. Montassier, R. Valdés-Mas, E. Batard, N. Zmora, M. Dori-Bachash, J. Suez, and E. Elinav,
636 “Probiotics impact the antibiotic resistance gene reservoir along the human GI tract in a person-
637 specific and antibiotic-dependent manner.,” *Nat. Microbiol.*, vol. 6, no. 8, pp. 1043–1054, Aug. 2021,

638 doi: 10.1038/s41564-021-00920-0.

639 [22] J.-P. Nougayrède, C. V Chagneau, J.-P. Motta, N. Bossuet-Greif, M. Belloy, F. Taieb, J.-J. Gratadoux,
640 M. Thomas, P. Langella, and E. Oswald, "A Toxic Friend: Genotoxic and Mutagenic Activity of the
641 Probiotic Strain Escherichia coli Nissle 1917.," *mSphere*, vol. 6, no. 4, p. e0062421, Aug. 2021, doi:
642 10.1128/mSphere.00624-21.

643 [23] M. Olier, I. Marcq, C. Salvador-Cartier, T. Secher, U. Dobrindt, M. Boury, V. Bacquié, M. Pénary, E.
644 Gaultier, J.-P. Nougayrède, J. Fioramonti, and E. Oswald, "Genotoxicity of Escherichia coli Nissle
645 1917 strain cannot be dissociated from its probiotic activity.," *Gut Microbes*, vol. 3, no. 6, pp. 501–
646 509, 2012, doi: 10.4161/gmic.21737.

647 [24] R. A. Oliveira, K. M. Ng, M. B. Correia, V. Cabral, H. Shi, J. L. Sonnenburg, K. C. Huang, and K. B.
648 Xavier, "Klebsiella michiganensis transmission enhances resistance to Enterobacteriaceae gut
649 invasion by nutrition competition.," *Nat. Microbiol.*, Jan. 2020, doi: 10.1038/s41564-019-0658-4.

650 [25] M. C. Collado, J. Meriluoto, and S. Salminen, "Role of commercial probiotic strains against human
651 pathogen adhesion to intestinal mucus.," *Lett. Appl. Microbiol.*, vol. 45, no. 4, pp. 454–460, Oct.
652 2007, doi: 10.1111/j.1472-765X.2007.02212.x.

653 [26] L. Osbelt, M. Wende, É. Almási, E. Derksen, U. Muthukumarasamy, T. R. Lesker, E. J. C. Galvez, M. C.
654 Pils, E. Schalk, P. Chhatwal, J. Färber, M. Neumann-Schaal, T. Fischer, D. Schlüter, and T. Strowig,
655 "Klebsiella oxytoca causes colonization resistance against multidrug-resistant K. pneumoniae in the
656 gut via cooperative carbohydrate competition.," *Cell Host Microbe*, vol. 29, no. 11, pp. 1663-
657 1679.e7, Nov. 2021, doi: 10.1016/j.chom.2021.09.003.

658 [27] J. Schluter, A. Djukovic, B. P. Taylor, J. Yan, C. Duan, G. A. Hussey, C. Liao, S. Sharma, E. Fontana, L. A.
659 Amoretti, R. J. Wright, A. Dai, J. U. Peled, Y. Taur, M.-A. Perales, B. A. Siranosian, A. S. Bhatt, M. R. M.
660 van den Brink, E. G. Pamer, *et al.*, "The TaxUMAP atlas: Efficient display of large clinical microbiome
661 data reveals ecological competition in protection against bacteremia," *Cell Host Microbe*, vol. 31, no.
662 7, pp. 1126-1139.e6, 2023, doi: https://doi.org/10.1016/j.chom.2023.05.027.

663 [28] R. D. Olson, R. Assaf, T. Brettin, N. Conrad, C. Cucinell, J. J. Davis, D. M. Dempsey, A. Dickerman, E.
664 M. Dietrich, R. W. Kenyon, M. Kuscuoglu, E. J. Lefkowitz, J. Lu, D. Machi, C. Macken, C. Mao, A.
665 Niewiadomska, M. Nguyen, G. J. Olsen, *et al.*, "Introducing the Bacterial and Viral Bioinformatics
666 Resource Center (BV-BRC): a resource combining PATRIC, IRD and ViPR.," *Nucleic Acids Res.*, vol. 51,
667 no. D1, pp. D678–D689, Jan. 2023, doi: 10.1093/nar/gkac1003.

668 [29] L. Craig, M. E. Pique, and J. A. Tainer, "Type IV pilus structure and bacterial pathogenicity.," *Nat. Rev.*
669 *Microbiol.*, vol. 2, no. 5, pp. 363–378, May 2004, doi: 10.1038/nrmicro885.

670 [30] P. Thiennimitr, S. E. Winter, M. G. Winter, M. N. Xavier, V. Tolstikov, D. L. Huseby, T. Sterzenbach, R.
671 M. Tsolis, J. R. Roth, and A. J. Bäumler, "Intestinal inflammation allows Salmonella to use
672 ethanolamine to compete with the microbiota.," *Proc. Natl. Acad. Sci. U. S. A.*, vol. 108, no. 42, pp.
673 17480–17485, Oct. 2011, doi: 10.1073/pnas.1107857108.

674 [31] C. Palmela, C. Chevarin, Z. Xu, J. Torres, G. Sevrin, R. Hirten, N. Barnich, S. C. Ng, and J.-F. Colombel,
675 "Adherent-invasive Escherichia coli in inflammatory bowel disease.," *Gut*, vol. 67, no. 3, pp. 574–
676 587, Mar. 2018, doi: 10.1136/gutjnl-2017-314903.

677 [32] A. G. Buret, J.-P. Motta, T. Allain, J. Ferraz, and J. L. Wallace, "Pathobiont release from dysbiotic gut
678 microbiota biofilms in intestinal inflammatory diseases: a role for iron?," *J. Biomed. Sci.*, vol. 26, no.
679 1, p. 1, Jan. 2019, doi: 10.1186/s12929-018-0495-4.

680 [33] J. P. 3rd Lynch, N. M. Clark, and G. G. Zhanel, "Escalating antimicrobial resistance among
681 Enterobacteriaceae: focus on carbapenemases.," *Expert Opin. Pharmacother.*, vol. 22, no. 11, pp.
682 1455–1473, Aug. 2021, doi: 10.1080/14656566.2021.1904891.

683 [34] N. A. Lerminiaux and A. D. S. Cameron, "Horizontal transfer of antibiotic resistance genes in clinical
684 environments.," *Can. J. Microbiol.*, vol. 65, no. 1, pp. 34–44, Jan. 2019, doi: 10.1139/cjm-2018-0275.

685 [35] G. Wang, G. Zhao, X. Chao, L. Xie, and H. Wang, "The Characteristic of Virulence, Biofilm and
686 Antibiotic Resistance of Klebsiella pneumoniae.," *Int. J. Environ. Res. Public Health*, vol. 17, no. 17,
687 Aug. 2020, doi: 10.3390/ijerph17176278.

688 [36] H. L. Mobley and R. P. Hausinger, "Microbial ureases: significance, regulation, and molecular
689 characterization.," *Microbiol. Rev.*, vol. 53, no. 1, pp. 85–108, Mar. 1989, doi: 10.1128/mr.53.1.85-
690 108.1989.

691 [37] M. Nakano, T. Iida, and T. Honda, "Urease activity of enterohaemorrhagic Escherichia coli depends
692 on a specific one-base substitution in ureD.," *Microbiology*, vol. 150, no. Pt 10, pp. 3483–3489, Oct.
693 2004, doi: 10.1099/mic.0.27280-0.

694 [38] S. Clegg and C. N. Murphy, "Epidemiology and Virulence of Klebsiella pneumoniae.," *Microbiol.*
695 *Spectr.*, vol. 4, no. 1, Feb. 2016, doi: 10.1128/microbiolspec.UTI-0005-2012.

696 [39] U. Sonnenborn and J. Schulze, "The non-pathogenic Escherichia coli strain Nissle 1917 – features of
697 a versatile probiotic," *Microb. Ecol. Health Dis.*, vol. 21, no. 3–4, pp. 122–158, Jan. 2009, doi:
698 10.3109/08910600903444267.

699 [40] R. Podschun, D. Sievers, A. Fischer, and U. Ullmann, "Serotypes, hemagglutinins, siderophore
700 synthesis, and serum resistance of Klebsiella isolates causing human urinary tract infections.," *J.*
701 *Infect. Dis.*, vol. 168, no. 6, pp. 1415–1421, Dec. 1993, doi: 10.1093/infdis/168.6.1415.

[41] C. Ronda, S. P. Chen, V. Cabral, S. J. Yaung, and H. H. Wang, “Metagenomic engineering of the mammalian gut microbiome in situ,” *Nat. Methods*, vol. 16, no. 2, 2019, doi: 10.1038/s41592-018-0301-y.

[42] A. S. Millan, R. Peña-Miller, M. Toll-Riera, Z. V Halbert, A. R. McLean, B. S. Cooper, and R. C. MacLean, “Positive selection and compensatory adaptation interact to stabilize non-transmissible plasmids,” *Nat. Commun.*, vol. 5, no. 1, p. 5208, 2014, doi: 10.1038/ncomms6208.

[43] A. Alonso-del Valle, R. León-Sampedro, J. Rodríguez-Beltrán, J. DelaFuente, M. Hernández-García, P. Ruiz-Garbajosa, R. Cantón, R. Peña-Miller, and A. San Millán, “Variability of plasmid fitness effects contributes to plasmid persistence in bacterial communities,” *Nat. Commun.*, vol. 12, no. 1, p. 2653, 2021, doi: 10.1038/s41467-021-22849-y.

[44] B. Chassaing, G. Srinivasan, M. A. Delgado, A. N. Young, A. T. Gewirtz, and M. Vijay-Kumar, “Fecal lipocalin 2, a sensitive and broadly dynamic non-invasive biomarker for intestinal inflammation.,” *PLoS One*, vol. 7, no. 9, p. e44328, 2012, doi: 10.1371/journal.pone.0044328.

[45] A. R. Moschen, T. E. Adolph, R. R. Gerner, V. Wieser, and H. Tilg, “Lipocalin-2: A Master Mediator of Intestinal and Metabolic Inflammation.,” *Trends Endocrinol. Metab.*, vol. 28, no. 5, pp. 388–397, May 2017, doi: 10.1016/j.tem.2017.01.003.

[46] M. Drouet, C. Vignal, E. Singer, M. Djouina, L. Dubreuil, A. Cortot, P. Desreumaux, and C. Neut, “AIEC colonization and pathogenicity: influence of previous antibiotic treatment and preexisting inflammation.,” *Inflamm. Bowel Dis.*, vol. 18, no. 10, pp. 1923–1931, Oct. 2012, doi: 10.1002/ibd.22908.

[47] A. Couturier-Maillard, T. Secher, A. Rehman, S. Normand, A. De Arcangelis, R. Haesler, L. Huot, T. Grandjean, A. Bressenot, A. Delanoye-Crespin, O. Gaillot, S. Schreiber, Y. Lemoine, B. Ryffel, D. Hot, G. Nùñez, G. Chen, P. Rosenstiel, and M. Chamaillard, “NOD2-mediated dysbiosis predisposes mice to transmissible colitis and colorectal cancer.,” *J. Clin. Invest.*, vol. 123, no. 2, pp. 700–711, Feb. 2013, doi: 10.1172/JCI62236.

[48] P. R. de Souza, F. R. Guimarães, H. Sales-Campos, G. Bonfá, V. Nardini, J. E. L. Chica, W. M. Turato, J. S. Silva, D. S. Zamboni, and C. R. de B. Cardoso, “Absence of NOD2 receptor predisposes to intestinal inflammation by a deregulation in the immune response in hosts that are unable to control gut dysbiosis.,” *Immunobiology*, vol. 223, no. 10, pp. 577–585, Oct. 2018, doi: 10.1016/j.imbio.2018.07.003.

[49] R. Lev-Tzion, O. Ledder, E. Shteyer, M. L. N. Tan, H. H. Uhlig, and D. Turner, “Oral Vancomycin and Gentamicin for Treatment of Very Early Onset Inflammatory Bowel Disease.,” *Digestion*, vol. 95, no.

4, pp. 310–313, 2017, doi: 10.1159/000475660.

[50] K. Aden, A. Rehman, S. Waschina, W.-H. Pan, A. Walker, M. Lucio, A. M. Nunez, R. Bharti, J. Zimmerman, J. Bethge, B. Schulte, D. Schulte, A. Franke, S. Nikolaus, J. O. Schroeder, D. Vandeputte, J. Raes, S. Szymczak, G. H. Waetzig, *et al.*, "Metabolic Functions of Gut Microbes Associate With Efficacy of Tumor Necrosis Factor Antagonists in Patients With Inflammatory Bowel Diseases.," *Gastroenterology*, vol. 157, no. 5, pp. 1279-1292.e11, Nov. 2019, doi: 10.1053/j.gastro.2019.07.025.

[51] A. Di Sabatino, P. Cazzola, R. Ciccocioppo, R. Morera, P. Biancheri, L. Rovedatti, L. Cantoro, A. Vanoli, F. P. Tinozzi, S. Tinozzi, and G. R. Corazza, "Efficacy of butyrate in the treatment of mild to moderate Crohn's disease," *Dig. Liver Dis. Suppl.*, vol. 1, no. 1, pp. 31–35, 2007, doi: https://doi.org/10.1016/S1594-5804(08)60009-1.

[52] J. Chen and L. Vitetta, "The Role of Butyrate in Attenuating Pathobiont-Induced Hyperinflammation.," *Immune Netw.*, vol. 20, no. 2, p. e15, Apr. 2020, doi: 10.4110/in.2020.20.e15.

[53] J. Connors, N. Dawe, and J. Van Limbergen, "The Role of Succinate in the Regulation of Intestinal Inflammation.," *Nutrients*, vol. 11, no. 1, Dec. 2018, doi: 10.3390/nu11010025.

[54] M. T. Sorbara, K. Dubin, E. R. Littmann, T. U. Moody, E. Fontana, R. Seok, I. M. Leiner, Y. Taur, J. U. Peled, M. R. M. van den Brink, Y. Litvak, A. J. Baumler, J.-L. Chaubard, A. J. Pickard, J. R. Cross, and E. G. Pamer, "Inhibiting antibiotic-resistant Enterobacteriaceae by microbiota-mediated intracellular acidification.," *J. Exp. Med.*, vol. 216, no. 1, pp. 84–98, Jan. 2019, doi: 10.1084/jem.20181639.

[55] A. Djukovic, M. J. Garzón, C. Canlet, V. Cabral, R. Lalaoui, M. García-Garcerá, J. Rechenberger, M. Tremblay-Franco, I. Peñaranda, L. Puchades-Carrasco, A. Pineda-Lucena, E. M. González-Barberá, M. Salavert, J. L. López-Hontangas, M. Á. Sanz, J. Sanz, B. Kuster, J.-M. Rolain, L. Debrauwer, *et al.*, "Lactobacillus supports Clostridiales to restrict gut colonization by multidrug-resistant Enterobacteriaceae.," *Nat. Commun.*, vol. 13, no. 1, p. 5617, Sep. 2022, doi: 10.1038/s41467-022-33313-w.

[56] K. Wilson, "Preparation of genomic DNA from bacteria.," *Curr. Protoc. Mol. Biol.*, vol. Chapter 2, p. Unit 2.4, Nov. 2001, doi: 10.1002/0471142727.mb0204s56.

[57] A. Reisner, K. A. Krogfelt, B. M. Klein, E. L. Zechner, and S. Molin, "In vitro biofilm formation of commensal and pathogenic Escherichia coli strains: impact of environmental and genetic factors.," *J. Bacteriol.*, vol. 188, no. 10, pp. 3572–3581, May 2006, doi: 10.1128/JB.188.10.3572-3581.2006.

[58] G. A. O'Toole, "Microtiter dish biofilm formation assay.," *J. Vis. Exp.*, no. 47, Jan. 2011, doi: 10.3791/2437.

[59] D. B. Alexander and D. A. Zuberer, "Use of chrome azurol S reagents to evaluate siderophore

766 production by rhizosphere bacteria," *Biol. Fertil. Soils*, vol. 12, no. 1, pp. 39–45, 1991, doi:
767 10.1007/BF00369386.

768 [60] S. Das and M. Barooah, "Characterization of siderophore producing arsenic-resistant Staphylococcus
769 sp. strain TA6 isolated from contaminated groundwater of Jorhat, Assam and its possible role in
770 arsenic geocycle," *BMC Microbiol.*, vol. 18, no. 1, p. 104, 2018, doi: 10.1186/s12866-018-1240-6.

771 [61] J. A. Thompson, R. A. Oliveira, A. Djukovic, C. Ubeda, and K. B. Xavier, "Manipulation of the Quorum
772 Sensing Signal AI-2 Affects the Antibiotic-Treated Gut Microbiota," *Cell Rep.*, vol. 10, no. 11, pp.
773 1861–1871, Mar. 2015, doi: 10.1016/j.celrep.2015.02.049.

774 [62] J. G. Caporaso, C. L. Lauber, W. A. Walters, D. Berg-Lyons, C. A. Lozupone, P. J. Turnbaugh, N. Fierer,
775 and R. Knight, "Global patterns of 16S rRNA diversity at a depth of millions of sequences per
776 sample," *Proc. Natl. Acad. Sci.*, vol. 108, no. supplement_1, pp. 4516–4522, Mar. 2011, doi:
777 10.1073/pnas.1000080107.

778 [63] J. G. Caporaso, C. L. Lauber, W. A. Walters, D. Berg-Lyons, J. Huntley, N. Fierer, S. M. Owens, J.
779 Betley, L. Fraser, M. Bauer, N. Gormley, J. A. Gilbert, G. Smith, and R. Knight, "Ultra-high-throughput
780 microbial community analysis on the Illumina HiSeq and MiSeq platforms," *ISME J.*, vol. 6, no. 8, pp.
781 1621–1624, 2012, doi: 10.1038/ismej.2012.8.

782 [64] E. Pruesse, C. Quast, K. Knittel, B. M. Fuchs, W. Ludwig, J. Peplies, and F. O. Glöckner, "SILVA: a
783 comprehensive online resource for quality checked and aligned ribosomal RNA sequence data
784 compatible with ARB.," *Nucleic Acids Res.*, vol. 35, no. 21, pp. 7188–7196, 2007, doi:
785 10.1093/nar/gkm864.

786 [65] B. J. Haas, D. Gevers, A. M. Earl, M. Feldgarden, D. V Ward, G. Giannoukos, D. Ciulla, D. Tabbaa, S. K.
787 Highlander, E. Sodergren, B. Methé, T. Z. DeSantis, J. F. Petrosino, R. Knight, and B. W. Birren,
788 "Chimeric 16S rRNA sequence formation and detection in Sanger and 454-pyrosequenced PCR
789 amplicons.," *Genome Res.*, vol. 21, no. 3, pp. 494–504, Mar. 2011, doi: 10.1101/gr.112730.110.

790 [66] Q. Wang, G. M. Garrity, J. M. Tiedje, and J. R. Cole, "Naive Bayesian classifier for rapid assignment of
791 rRNA sequences into the new bacterial taxonomy.," *Appl. Environ. Microbiol.*, vol. 73, no. 16, pp.
792 5261–5267, Aug. 2007, doi: 10.1128/AEM.00062-07.

793 [67] J. Barroso-batista, M. F. Pedro, J. Sales-dias, and C. J. G. Pinto, "Specific eco-evolutionary contexts in
794 the mouse gut reveal Escherichia coli metabolic versatility."

795

796

797 **Figure Legends**

798

799 **Fig. 1 | ARO112 genomic comparison with other *Enterobacteriaceae* strains from the *Klebsiella* and**
800 ***Escherichia* genera for their pathogenic potential. a,** Phylogenetic tree based on whole-genome analysis of
801 15 strains (5 *E. coli* strains, 5 *K. pneumoniae* strains, and 5 non-*pneumoniae Klebsiella* strains). Strains in bold
802 were tested experimentally; detailed description of the different the strains in Supplementary Table 1. **b,**
803 Heatmap, **c,** Principal Coordinate Analysis representing presence/absence of pathogenic properties and **d,**
804 Principal Coordinate Analysis of the different strains using the abundance of pathogenic properties. **c-d,**
805 ellipses represent 90% confidence.

806

807 **Fig. 2 | Phenotypical evaluation of ARO112 and other *Enterobacteriaceae* strains for nosocomial-**
808 **related pathogenic factors important for host invasion and colonization. a**, Schematic representation of the
809 pipeline used to test bacterial strains for pathogenic traits. A set of 9 strains (4 *E. coli*, 3 *K. pneumoniae*, 2
810 non-*pneumoniae Klebsiella*) were tested, both in rich and minimal media, for: **b,** antibiotic resistance, MDR
811 *Enterobacteriaceae* strains are represented in bold (resistant to >3 classes of antibiotics); **c,** biofilm
812 formation; **d,** urease activity; **e,** siderophore production; and **f,** capacity to resist killing or inhibition by human
813 serum. Selected strains (ARO112, EcN, and Kp1012) were tested for their capacity to **g**, acquire the
814 conjugative plasmid RP4 from MG1655 donor strain or Kgri donor strain, or **h**, retain the plasmid in rich and
815 minimal media. **i**, The capacity to retain the non-conjugative plasmid pMP7605 in rich and minimal media
816 was also tested. In **c**-**i**, bars represent median values. **b,** includes data from a total of 6 replicates per group,
817 from 2 independent experiments; **c**, from a total of 15 replicates per group, from 3 independent experiments;
818 **d**, from a total of 6 replicates per group, from 2 independent experiments; **e,** more than 8 replicates per
819 group, from 3 independent experiments; **f,** from a total of 6 replicates per group, from 2 independent
820 experiments; **g,** from a total of 15 (from MG1655 RP4) or 10 (From Kgri RP4) replicates per group, from 2-4
821 independent experiments; **h,** from a total of 6 replicates per group, from 2 independent experiments; **i,** a
822 total of 7 replicates per group, from 2 independent experiments. In **c-g,** statistical analysis was done using
823 Kruskal-Wallis' test with Dunn's correction for multiple comparisons. In **e-f,** different letters denote
824 significant differences among strains within the same medium ($p<0.05$) and # denotes significant differences
825 between different media for the same strain ($p<0.05$). In **h** and **i**, data were analyzed using Two-way ANOVA
826 with Sidak's correction for multiple comparisons. * $p<0.05$; ** $p<0.01$; **** $p<0.0001$.

827

828

829 **Fig. 3 | Phenotypic testing of ARO112, EcN, and Kp1012 isolated from fecal samples of mono-**
830 **colonized mice. a**, Schematic representation of the pipeline used to test bacterial strains for pathogenic traits
831 after gut colonization. Germ-free (GF) mice were mono-colonized with each of selected strains (ARO112, EcN,
832 Kp1012) for five days, after which bacteria were isolated from the fecal samples and tested for **b,** urease
833 activity and **c,** resistance to human serum. **d,** Bacteria were also evaluated for plasmid retention upon
834 intestinal colonization. **e,** Fecal supernatants were evaluated for Lipocalin-2/NGAL levels, as a marker for
835 intestinal inflammation. In **b**-**e**, data were analyzed using Kruskal-Wallis' test with Dunn's correction for
836 multiple comparisons (* $p<0.05$; ** $p<0.01$; **** $p<0.0001$). Urease activity and human serum resistance
837 from gut isolated bacteria were tested in a total of 10 (ARO112), 8 (EcN), or 4-7 (Kp1012) replicates, from at
838 least 2-3 independent experiments. Lcn2 was tested in germ-free animals before colonization (GF, N= 24),
839 and after colonization with ARO112 (N=10), EcN (N=9), or Kp1012 (N=15), from at least 3 independent
840 experiments. Non-conjugative plasmid retention in gut-isolated bacteria was tested in a total of 10 (ARO112),
841 9 (EcN), or 7 (Kp1012) replicates, from at least 3 independent experiments. In **b**-**e**, bars and lines represent
842 median values.

843

844 **Fig. 4 | Evaluation of therapeutical potential capacities of ARO112 and EcN against AIEC**
845 **colonization in an IBD mouse model previously treated with antibiotics. a,** Experimental setup of IBD mouse
846 model Nod2$^{-/-}$ mice treated with antibiotics, followed by AIEC infection and treated with ARO112, EcN or PBS
847 (Ctrl). **b,** Percentage of mice colonized with AIEC in the different groups throughout the experiment. **c,** AIEC
848 loads during the experiment. Thin lines represent AIEC loads in individual mice over time, while thick lines
849 represent median values for each treatment over time. In **b** and **c**, data were analyzed using Two-way ANOVA
850 with Tukey's correction for multiple comparisons (* $p<0.05$; ** $p<0.01$; **** $p<0.0001$). AIEC fecal loads and
851 colonization were tested in a total of 15 (Ctrl), 12 (+ARO112), or 10 (+EcN) animals, from 2-3 independent
852 experiments.

853

854 **Fig. 5 | Intestinal microbiota composition resultant from treatment with probiotic strains (ARO112,**
855 **EcN) or lack thereof (Ctrl). a,** Richness and **b,** diversity of gut microbiota in fecal samples collected before
856 (pre-AB, day -4), or after (post-AB, day 0) antibiotic treatment and 5 and 20 days after AIEC infections of mice
857 untreated (Ctrl) or treated with ARO112 or EcN. In **a** and **b**, lines represent median values for each treatment
858 over time. **c,** Changes in the relative abundances of most prevalent taxa at day 20 after AIEC infection in
859 comparison with the levels before antibiotics (day -4). **d,** Changes in relative abundances of potential butyrate
860 producers at day 5 after AIEC infection that were depleted by antibiotics, but recovered during experiment.
861 In **c** and **d**, different colors display severely depleted (<-5), depleted (<-1), unchanged or recovered (-1 to 1),

862 enriched (>1) and severely enriched (>5) log_2 fold changes to pre-AB levels of each mouse. In **a**-**d**, data were
863 analyzed using Two-way ANOVA with Dunnett's correction for multiple comparisons (* p<0.1; ** p<0.01; ***
864 p<0.001; **** p<0.0001). Fecal microbiota composition analyses were performed in a total of 14 (Ctrl), 10
865 (+ARO112), or 4-10 (+EcN) samples, from 2-4 independent experiments.

866

867 **Fig. 6 | SCFA levels and intestinal inflammation profiles of mice upon different probiotic treatments**
868 **(ARO112, EcN) or lack thereof (Ctrl). a,** Metabolomic profile of butyrate, isobutyrate, acetate, propionate,
869 and succinate in fecal samples of IBD mouse model Nod2$^{-/-}$ mice not treated (Ctrl) or treated with probiotics
870 ARO112 (+ARO112) or EcN (+EcN), at the end of the experiment. **b,** Intestinal inflammation was measured
871 via Lcn2 proxy in fecal supernatants, throughout the experiment. Thin lines represent Lcn2 levels in individual
872 mice overtime, while thick lines represent median values for each treatment overtime. In **a**, bars represent
873 median values and data were analyzed using Kruskal-Wallis test with Dunn's correction for multiple
874 comparisons. In **b**, data were analyzed using Two-way ANOVA with Tukey's correction for multiple
875 comparisons (* p<0.05; ** p<0.01; *** p<0.001; **** p<0.0001). Metabolomics and Lcn2 were tested in 12
876 (Ctrl), 8 (+ARO112) and 10 (+EcN) samples.

877

878

879 **Extended Data Figures Legends**

880

881 **Extended Data Fig. 1 | Quantification and comparison of genome-encoded gene products and**
882 **predicted virulence factors' properties.** Genome analyses were performed in PATRIC BV-BRC software, from
883 where the number of hits for the different virulence factors databases were obtained. **a,** Venn diagram of
884 total gene products, shared by every member of each clade and Venn diagram of virulence properties' hits
885 shared by every member of each clade. **b,** Number of gene products encoded on the genome of each strain
886 related to each of 8 clinically-relevant categories, per clade. In **c**, data were analyzed using Two-way ANOVA
887 with Tukey's correction for multiple comparisons (* p<0.05; ** p<0.01; **c**).

888

889 **Extended Data Fig. 2 | Comparison and correlations of phenotypically tested virulence traits. a,**
890 Bacterial growth in rich and minimal media. **b,** ARO112 and EcN were tested for their capacity to retain a
891 natural antibiotic-resistant plasmid acquired by conjugation from the clinical isolate Kp834. In **a** and **b**, bars
892 represent median values. In **b**, data were analyzed using Two-way ANOVA test with Sidak's correction for
893 multiple comparisons (**p<0.01; **** p<0.0001). Growth was tested in 6-11 replicates, from 2 independent

894 experiments. Natural conjugative plasmid retention was tested in a total of 5 replicates per group, from 2
895 independent experiments.

896

897 **Extended Data Fig. 3 | Siderophore production in mono-colonized mice and resistance to Lcn2. a,**
898 Siderophores were measured in fecal supernatants collected from mice mono-colonized with each of
899 selected strains (ARO112, EcN, Kp1012) for 5 days. Bars represent median values. **b**, Selected strains
900 (ARO112, EcN, Kp1012) were tested for their capacity to grow in the presence of increased concentrations of
901 Lcn2 in rich or minimal media. Growth capacity was categorized as resistant (>80%), intermediate (>40%), or
902 sensitive (<40%) when compared to the absence of Lcn2. In **a**, siderophore production in fecal samples was
903 tested in a total of 10 (ARO112), 9 (EcN), or 7 (Kp1012) samples, from at least 3 independent experiments. In
904 **b**, Lcn2 resistance was tested in a total of 6 replicates, from 2 independent experiments.

905

906 **Extended Data Fig. 4 | Probiotic colonization and evaluation of protective capacities of ARO112**
907 **and EcN against different invading bacteria in different mouse models. a,** Loads of AIEC in fecal samples of
908 WT mice treated with vancomycin and gentamicin and treated with PBS (Ctrl) or ARO112 probiotic
909 (+ARO112). **b-c,** data from experiment shown in Fig. 4, where **b,** shows the loads of ARO112 or EcN in fecal
910 samples and **c,** the percentage of mice colonized by ARO112 or EcN during (13 timepoints tested) the
911 experiment in Nod2$^{-/-}$ mice. **d,** Loads of AIEC in fecal samples of WT mice treated with streptomycin and
912 treated with ARO112 (+ARO112) or EcN (+EcN) probiotics. **e,** Loads of AIEC in germ-free WT mice treated
913 with PBS (Ctrl) or ARO112 probiotic (+ARO112). Loads of **f,** Ec1898, **g,** *V. cholerae***,** and **h,** Kp1012 after 4 days
914 of mono-colonization (pre-treat) or after 8 days of treatment with ARO112 (+ARO112), in germ-free WT mice.
915 **i,** Loads of AIEC after 24h of growth without or with ARO112 or EcN, in rich or minimal media. AIEC loads in
916 WT SPF models were tested in 3 replicates per group (**a**) or 7 replicates per group (**d**), from 1 or 2 independent
917 experiments, respectively. Probiotic loads were tested in 12 (+ARO112) or 10 (+EcN) replicates from 2-3
918 independent experiments (**b**). AIEC loads in WT GF model were tested in 3 (Ctrl) and 9 (+ARO112) replicates
919 in 1-2 independent experiments (**e**). Ec1898 loads were assessed in 5 replicates from 2 independent
920 experiments (**f**). *V. cholerae* loads were assessed from 6 replicates from 2 independent experiments (**g**).
921 Kp1012 loads were assessed in 8 replicates from 2 independent experiments (**h**). In vitro growths were tested
922 in 10 (Ctrl), 7 (+ARO112), or 3 (+EcN) replicates in minimal medium, and 9 (Ctrl), 19 (+ARO112), or 19 (+EcN)
923 replicates in rich medium, from 1-4 independent experiments (**i**), and two-way ANOVA was tested with
924 Tukey's multiple comparison correction (* $p<0.05$; **** $p<0.0001$). In f-h, data were analyzed using Mann-
925 Whitney tests (* $p<0.05$; *** $p<0.001$). In **b**, thin lines represent ARO112 and EcN loads in individual mice
926 over time, while in **a**, **b**, **d**, **e**, thick lines and bars represent median values.

927

928 **Extended Data Fig. 5 | Comparison between treatments of different microbiota-related**
929 **parameters in experiment in Nod2$^{-/-}$ mice. a,** Principal Coordinate Analysis displaying clustering of samples
930 before antibiotic treatment (pre-AB; 33 samples), after antibiotic treatment (post-AB; 34 samples), and after
931 treatment with PBS (Ctrl; 14 samples) or probiotics (+ARO112 or +EcN; 10 samples per group), using
932 microbiota composition or **b,** selective four potential butyrate producers (*Dorea*, *Oscillibacter*,
933 unc_*Runimococcacea*, unc_*Lachnospiraceae*). Ellipses in **a** and **b** represent 90% confidence intervals. **c,**
934 Relative abundance of Pseudomonadota taxon enriched after antibiotic treatment. Values were tested from
935 14 (Ctrl), 11 (+ARO112) or 4-10 (+EcN) mice. In **c**, lines represent median values and data were analyzed using
936 Two-way ANOVA with Tukey's correction for multiple comparisons.

937

938

939 **Material and Methods**

940 Bacterial strains, plasmids and culture conditions

941 See Supplementary Table 1 for all species, strains, and plasmids. Unless otherwise specified bacteria
942 were cultured in Lysogenic Broth (LB, here refereed as rich medium) or M9 minimal medium (47.74mM
943 $NaHPO_4$-$7H_2O$, 22.04mM KH_2PO_4, 8.554mM NaCl, 18.694mM NH_4Cl, 2mM $MgSO_4$, 0.1mM $CaCl_2$, 1mM
944 thiamine) with 0.5% glucose media at 37ºC with aeration (shaking at 240 rpm).

945 Whole genome sequencing

946 One *Klebsiella oxytoca* MBC022 clone was isolated from the feces of a WT specific pathogen-free
947 (SPF) C57BL/6J mice bred in the animal house facility at Instituto Gulbenkian Ciência and grown in LB at 37
948 °C with agitation for subsequent DNA isolation using a previously described protocol [56]. A DNA library was
949 constructed and sequenced at the IGC Genomics facility. Paired-end sequencing of each sample was
950 performed using an Illumina MiSeq Benchtop Sequencer (Illumina), which produced datasets of 250 bp read
951 pairs. *K. oxytoca* genome has been deposited in GenBank (see Data availability).

952 Ec1898, Kp1012, and Kp834 were isolated from leukemia patients from Hospital La Fe in Valencia
953 (Spain). Genome sequence was obtained as described above in the FISABIO Sequencing facility. Sequences
954 have been deposited in GenBank.

955 Method for phylogenetic tree

956 Phylogenetic tree was performed using the whole genomes of strains uploaded to the PATRIC BV-
957 BRC browser software (v3.29.20). Parameters used included 100 single-copy genes, using Multiple Alignment
958 using Fast Fourier (MAFFT) Transform alignment program and RAxML Fast Bootstrapping branch support
959 method (v8.2.11).

960 Genome-encoded predicted pathogenic properties

961 Genomes of all strains were uploaded to the PATRIC BV-BRC [28] browser software (v3.29.20) and
962 analyzed. For each genome, a table containing all predicted pathogenic properties from 9 available
963 databases: 3 for Virulence Factors (Victors, PATRIC_VF, VFDB), 3 for Drug Targets and Transporters
964 (DrugBank, TCDB, TTD), and 3 for antibiotic resistance (PATRIC, CARD, NDARO). The ensemble of these data
965 was downloaded and two merged tables were compiled with the information for all the strains: one
966 displaying the presence or absence of each pathogenic property in each strain, and another including the
967 abundance of each pathogenic property in each strain. Principal Coordinates analyses were performed using
968 either presence/absence of pathogenic properties (Bray-Curtis dissimilarity index for binary/categorical data;
969 one-way PERMANOVA with Bonferroni correction) or abundance of said pathogenic properties (Euclidean
970 distances for continuous data; one-way PERMANOVA with Bonferroni correction).

971 Antibiotic profile

972 Cultures were grown in either rich or minimal medium for 24h at 37ºC with shaking. Cultures were
973 washed once in sterile PBS and adjusted to a final OD_{600} of 0.05 in 150µl/well in the appropriate medium with
974 different concentrations of antibiotics (as specified). These cultures were then grown for 24h in a 96-well
975 plate in a plate shaker, after which OD_{600} measurements were performed in a plate reader Multiskan Sky.
976 Strains were considered resistant if in the presence of antibiotic could reach at least 80% of the growth
977 obtained in the absence of antibiotic. If growth in the presence of antibiotic was more than 40% and less
978 than 80% of the control growth, the strain was considered intermediate for resistance, and sensitive if grown
979 less than 40% of control growth. Resistance or intermediate resistance to one antibiotic of any class is
980 considered resistance or intermediate resistance to that class of antibiotics. Sensitivity to a class of antibiotics
981 means that bacteria were sensitive to all antibiotics tested of that class. A strain was considered multidrug
982 resistant (MDR) if it was non-susceptible (sensitive or intermediate) to at least 1 antimicrobial agent in 3 or
983 more antimicrobial classes, in both tested media, as defined before [55].

Class	Antibiotic	Concentration (µg/ml)
β-lactam	ampicillin	100
	carbenicillin	50
Aminoglycosides	streptomycin	100
	kanamycin	50
	gentamicin	15
	neomycin	200
	apramycin	50
	spectinomycin	50
Chloramphenicol	chloramphenicol	25
Macrolides	erythromycin	125
Rifamycins	rifampicin	20
Tetracyclines	tetracycline	10
Fluoroquinolones	ciprofloxacin	0.5
	trimethoprim	4

Naphthyridone	nalidixic acid	32
Cephalosporins	cefotoxidine	8

984

985 Biofilm formation

986 Biofilm formation assays were performed by adapting a previously published method [57], [58]. In
987 summary, bacterial cultures were grown for 24h in either rich or minimal media at 37ºC with shacking. The
988 following day, each culture was washed once in sterile PBS, and final OD_{600} adjusted to 0.05 in the appropriate
989 medium and 200 μl of culture were dispensed per well in 48-well plates. Plates were centrifuged for 5 min at
990 4000 rpm at room temperature, after which plates were incubated at 37ºC for 90 min for adhesion. After
991 adhesion, supernatants were carefully removed and discarded, wells were washed once with 200 μl of sterile
992 PBS, and 500 μl of sterile fresh appropriate medium were carefully dispensed per well. Plates were incubated
993 at 37ºC for 24h, after which attached biofilms (biomass) was quantified with Crystal Violet (CV). For that
994 supernatants were removed and discarded and well bottoms were carefully washed with 500 μl of sterile
995 PBS. Each well was carefully stained with 0.1% CV solution and plates were incubated at room temperature
996 for 20 min protected from light. After incubation, each well was washed with PBS and plates were incubated
997 open and inverted in a paper towel for 30 min protected from light, to dry. Each well was then de-stained
998 with 200μl of a 33% glacial acetic acid solution and incubated for 15 min at room temperature protected
999 from light. Supernatants were removed from each well into a new plate and read for OD_{580} in a Multiskan Sky
1000 plate reader (peak for CV staining), to quantify biofilm biomass.

1001 Urease activity

1002 Cultures were grown in either rich or minimal medium for 24h at 37ºC with shaking. Cultures were
1003 washed once in sterile PBS and adjusted to an OD_{600} of 1, after which each culture was diluted 20x in urea
1004 medium (3g/L L-tryptophan, 5 g/L NaCl, 1g/L H_2KO_4P, 1g/L $H_2K_2O_4P$, 20g/L urea, 0,012g/L phenol red) and
1005 incubated for 24h at 37ºC with shaking. Urea degradation leads to the medium color to change from
1006 yellow/orange to pink/red. 100 μl of each culture were then transferred into a 96-wellplate and measured
1007 at OD_{560} in a Multiskan Sky plate reader to quantify urease activity. For urease activity measurement of
1008 bacteria extracted from fecal samples of monocolonized mice, cell suspensions of $2.5x10^7$ cells/ml were used,
1009 instead of the grown culture.

1010 Siderophore production

1011 Cultures were grown in either rich or minimal medium for 24h at 37ºC with shaking. Cultures or fecal
1012 samples diluted in PBS were centrifuged to recover supernatants. Culture and fecal supernatants were
1013 filtered in 0.22 μm filters. Cell-free supernatants (100 μl) were mixed 1:1 (v:v) with Cas-PIPES solution (100

1014 μl) [59], [60] in a 96-well plate and incubated at room temperature for 20 min, after which OD_{630} was
1015 measured in Multiskan Sky plate reader to calculate percentage of siderophore production, using sterile
1016 media or PBS as reference.

1017 $$\%\ siderophores = \frac{(ref - sample) * 100}{ref}$$

1018 Resistance to pooled human serum

1019 Bacterial susceptibility to human serum was tested as described [40] with modifications. Bacterial
1020 strains were grown in either rich or minimal medium for 24h at 37ºC with shaking, or extracted directly from
1021 fecal pellets. Cultures were washed once in sterile PBS and adjusted to $2x10^7$ cells/ml, after which 25 μl of
1022 cell suspension in PBS were added to 75 μl of pooled human serum solution (P30-2401, PAN-Biotech).
1023 Cultures were plated in LB agar plates for CFUs at 0h and after 3h of static incubation at 37ºC, to assess killing,
1024 resistance, or proliferation of bacterial cells in the presence of human serum.

1025 Plasmid conjugation

1026 Cultures were grown in rich medium for 24h at 37ºC with shaking. Cultures were washed once in
1027 sterile PBS. Donor (MG1655 RP4/RK2, Kgri RP4/RK2) and recipient (ARO112, EcN, Kp1012) strains were
1028 thoroughly mixed at a 1:1 ratio (total of 10^8 cells), centrifuged for 30 sec at 14,000 rpm and resuspended in
1029 20 μl of PBS. Two drops of 10 μl each were placed on an agar plate, air-dried, and incubated at 37ºC for 24h.
1030 After incubation, both drops were removed with a sterile loop and resuspended in 1 ml of sterile PBS. Serial
1031 dilutions were performed and plated to count CFUs for recipient strain with (selective plating with plasmid-
1032 borne antibiotic resistance) and without (non-selective or selective plating for recipient's antibiotic resistance
1033 plating) tested plasmid. Conjugative plasmid (RP4) harbors resistance to tetracycline (10 μg/ml) and
1034 kanamycin (50 μg/ml).

1035 Plasmid retention

1036 Strains harboring tested plasmids (RP4 acquired through conjugation from MG1655 RP4 donor strain;
1037 pMP7605 acquired through electroporation; Kanamycin resistance-bearing natural plasmid acquired through
1038 conjugation from Kp824) were grown in either rich or minimal medium with antibiotics (for plasmid-borne
1039 antibiotic resistance; kanamycin (50 μg/ml) and tetracycline (10 μg/ml) for RP4; gentamicin (30 μg/ml) for
1040 pMP7605; kanamycin (50 μg/ml) for natural plasmid) for 24h at 37ºC with shaking. Cultures were washed
1041 once in sterile PBS and adjusted to a final OD_{600} of 0.05 in 150 μl in the appropriate medium without
1042 antibiotics, and serial dilutions were plated in selective and non-selective LB agar plates, to assess CFUs with
1043 (plasmid retention) and without (plasmid loss) antibiotic resistance. Cultures were incubated at 37ºC with

1044 shaking for 24h. Every 24h, cultures were diluted 1:100 in fresh appropriate medium and re-incubated. After
1045 5 days of passages, serial dilutions of cultures were plated as mentioned before.

1046 Animal experimentation

1047 All of the mouse experiments performed at Instituto Gulbenkian Ciência (IGC) were approved by the
1048 Institutional Ethics Committee and the Portuguese National Entity (Direção Geral de Alimentação e
1049 Veterinária; 015190), which complies with European Directive 86/609/EEC of the European Council.

1050 C57BL/6J male mice, either WT or Nod2$^{-/-}$, were used at 6–8 weeks of age and were randomly
1051 assigned to experimental and control groups. C57BL/6J mice were used for all experiments. None of the
1052 animal experiments were performed blinded. Sample size was chosen according to institutional directives
1053 and in accordance with the guiding principles underpinning humane use of animals in research. No statistical
1054 analyses were performed to predetermine the sample sizes. All of the experiments were performed at least
1055 twice, except when stated otherwise.

1056 Fecal bacterial extraction

1057 WT C57BL/6J germ-free mice were orally gavaged with 100 µL containing ~10^8 CFUs of ARO112, EcN,
1058 or Kp1012 strains bearing the non-conjugative plasmid pMP7605. Five days later, fecal pellets were collected
1059 for live gut bacteria extraction, as previously described [41]. Briefly, pellets were weighed and 500 µL of
1060 sterile PBS were added before mechanical disruption with a motorized pellet pestle, after which another 500
1061 µL of sterile PBS were added. Samples were subjected to four iterations of vortex mixing for 15 sec,
1062 centrifugation at 1,000 rpm for 30 sec at room temperature and recovery of 750 µL of the debris-free cell-
1063 containing supernatants into a new tube, replacing that volume with sterile PBS before the next iteration.
1064 After recovery of 3 ml per sample, isolated cells were centrifuged at 4,000 g for 5 min at room temperature,
1065 discarding the supernatant and resuspending the cells fractions in 1 ml of sterile PBS supplemented with
1066 glycerol and cysteine at final concentrations of 20% and 0.1%, respectively. Samples were frozen and stored
1067 at -80ºC, to measure the phenotypes listed below.

1068 Nod2$^{-/-}$ and WT SPF mice experiments

1069 C57BL/6J Nod2$^{-/-}$ and WT mice bred under specific pathogen-free conditions in the animal house
1070 facility at the Instituto Gulbenkian Ciência were kept individually in sterile ISOcages (Tecniplast) at our specific
1071 opportunistic pathogen-free facility. Mice were orally gavaged with gentamicin (3 mg/kg/d) and vancomycin
1072 (40 mg/kg/d) once daily for three consecutive days [46]. Two days after the last gavage with antibiotics, mice
1073 were orally gavaged with 100µL containing ~10^8 CFUs of AIEC strain (LF82-strepR), and the following day were
1074 orally gavaged either with 100 µL of PBS (control), or 100 µL containing ~10^8 CFUs of ARO112 or EcN strains.
1075 Fecal samples were collected at the timepoints indicated in the corresponding graph and plated in selective

1076 medium to assess colonization levels of AIEC. Additionally, fecal samples were also used to measure levels of
1077 Lcn2 (Lipocalin-2/NGAL ELISA) and to assert the intestinal microbiota composition.

1078 C57BL/6J WT mice bred under SPF conditions in the animal house facility at the Instituto Gulbenkian
1079 Ciência were kept individually in ventilated cages with high-efficiency particulate air filters in our animal
1080 facility. Streptomycin (5 g/l) was maintained ad libitum in the drinking water for 15 days, being replaced every
1081 3 days, after which mice were kept in non-supplemented water. Four days after halting streptomycin
1082 treatment, AIEC strain (LF82-strepR) was orally gavaged (~10^8 CFUs/mouse in 100 µL). Three days after that,
1083 either ARO112 strain or EcN strain were orally gavaged (~10^8 CFUs/mouse in 100 µL). Fecal samples were
1084 collected at the timepoints indicated in the corresponding graph and plated in selective medium to assess
1085 colonization levels of AIEC.

1086 WT gnotobiotic mice experiments

1087 C57BL/6J germ-free mice were bred and raised in IGC's Gnotobiology Unit in axenic isolators (La
1088 Calhene/ORM) and were later transferred into sterile ISOcages (Tecniplast). Animals were individually
1089 housed and orally gavaged with 100 µL containing ~10^8 CFUs of AIEC (LF82-strepR), Kp1012, *V. cholerae*, or
1090 Ec1898 strains. The following day, mice were gavaged with 100 µL containing ~10^8 CFUs of either ARO112 or
1091 EcN strains, or 100µl of PBS. Fecal samples were collected at the timepoints indicated in the corresponding
1092 graphs and plated in selective media to assess colonization levels of AIEC, Kp1012, *V. cholerae*, or EC1898
1093 strains.

1094 16S rRNA sequencing

1095 All fecal samples from SPF mice experiments stored at −80 °C were processed for DNA extraction as
1096 previously described [61]. In brief, DNA was extracted using a combination of the QIAamp Fast DNA Stool
1097 Mini Kit (Qiagen) according to the manufacturer's instructions, mechanical disruption using a motorized
1098 pellet pestle and elution to a final volume of 100 µL in ATE buffer. For each sample, the 16S rRNA gene was
1099 amplified using the 515F/806R (V4 regions) primer pairs recommended by the Earth Microbiome Project
1100 under the following PCR cycling conditions: 94 °C for 3 min; 35 cycles of 94°C for 60s, 50°C for 60s and 72°C
1101 for 105s; and extension at 72°C for 10min [62], [63]. After library preparation, 2 × 250 bp sequencing was
1102 performed at the IGC Genomics Unit using an Illumina MiSeq Benchtop Sequencer.

1103 Fecal microbiota analysis

1104 Mothur v.1.32.1 was used to process sequences as previously described [61], with some
1105 modifications. Sequences were converted to FASTA format. Sequences that were shorter than 220 bp
1106 containing homopolymers of longer than 8 bp or undetermined bases with no exact match with the forward
1107 and reverse primers, and barcodes that did not complement each other or that did not align with the

1108 appropriate 16S rRNA variable region, were not included in the analysis. A quality score above 30 (range, 0
1109 to 40, where 0 represents an ambiguous base) was used to process sequences, which were trimmed using a
1110 sliding-window technique over a 50 bp window. Sequences were trimmed from the 3' end until the quality
1111 score criterion was met, and were merged after that. Between 20,000 and 50,000 sequences were obtained
1112 per sample. 16S rRNA gene sequences were aligned using SILVA template reference alignment [64].
1113 ChimeraSlayer [65] was used to remove potential chimeric sequences. Sequences with distance-based
1114 similarity of greater than 97% were joined into the same OTU using the average-neighbour algorithm. All of
1115 the samples were rarefied to the same number of sequences (10,000) for diversity analyses. Samples below
1116 10,000 reads were removed from the analysis. A Bayesian classifier algorithm with a 60% bootstrap cut-off
1117 was used for each sequence [66]; sequences were assigned to the genus level where possible or otherwise
1118 to the closest genus-level classification. All OTUs were used, and taxa plotted are the result of the merge of
1119 OTUs with the same classification, being collapsed to 37 different taxa, with lower represented OTUs/taxa
1120 being summed and plotted as "other". Principal Coordinate Analyses were performed using the 37 taxa or a
1121 subset of 4 taxa of potential butyrate producers (*Dorea*, *Lachnospiraceae*, *Oscillibacter*, *Ruminococcaceae*),
1122 representing the Bray-Curtis dissimilarity index (one-way PERMANOVA with Bonferroni correction).

1123 SCFA quantification

1124 We performed 1H-NMR (proton nuclear magnetic resonance) analysis on fecal contents to determine
1125 the abundance of SCFA in the mouse gut of Nod2$^{-/-}$ treated with ARO112 and EcN, or untreated (control), as
1126 previously described [67]. Fecal samples (1 to 3 fecal pellets) were diluted in 1mL of PBS. To remove large
1127 debris, the samples were pelleted by centrifugation at 18000 g for 15 min at 4°C. Supernatant was collected
1128 and filtered through a 0.22 mm filter (Milipore). Next, samples were filtered with 3 KDa filters (Vivaspin 500)
1129 by centrifugation at 15000 g and 4°C, for 3 h (or until 150 µL of filtrate was obtained). Filtered samples were
1130 stored at −80°C until spectrum acquisition. For spectrum acquisition, samples were thawed at room
1131 temperature and 150 µL mixed with 60 µL of 350 mM phosphate buffer (pH 7.09 with 2% NaN3, 10 mL of a
1132 0.05% (w/v) 3-(Trimethylsilyl)propionic-2,2,3,3-d4 (TSP-d4, Sigma-Aldrich) solution, and 380 µL of deuterated
1133 water - D_2O) to a total volume of 600 µL. The mixture was transferred to a 5 mm glass NMR tube. All solutions
1134 were prepared with D_2O. Samples were homogenized by inversion and the spectra were acquired after pH
1135 measurement. Acquisitions were performed on a Bruker NEO 500MHz instrument equipped with QXI H-
1136 C/N/P 5 mm probe-head with z-gradients. 1H-NMR spectra were acquired using 1D NOESY pulse sequence
1137 with pre-saturation (noesypr1d) under the following conditions: 90 pulse for excitation mixing time 100 ms,
1138 acquisition time 4 s, and relaxation delay 1 s. All spectra were acquired with 200 scans at 25C, with 48018
1139 data points and 6002 Hz (12 ppm) spectral width (Chenomx acquisition parameters). The recorded 1H-NMR
1140 spectra were phase corrected using Bruker TopSpin 4.0.7 and spectra were then analyzed using Chenomx

1141 NMR Suite 8.1. Compounds were identified by manually fitting reference peaks to spectra in database
1142 Chenomx 500 MHz Version 10. Quantification was based on internal standard peak integration (TSP-d4).

1143 Graphical representation and Statistical analyses

1144 Phylogenetic tree (Fig. 1a) was done using iTOL (itol.embl.de). Cluster heatmap (Fig. 1b) was done
1145 using SRPlot (https://www.bioinformatics.com.cn), using bidirectional clustering, complete cluster method
1146 and Euclidean distances. All statistical graphs and statistical analyses presented were done using Graphpad
1147 Prism 8. Correlation tables (Extended Data Fig. 2 and 5) were drawn in Microsoft Excel for Mac, using results
1148 obtained with Graphpad Prism 8. Principal Coordinates analyses (Fig. 1, Extended Data Fig. 5) were obtained
1149 with Past4.02 software (https://folk.universitetetioslo.no/ohammer/past) as explained above.

1150

1151

1152

Fig. 1

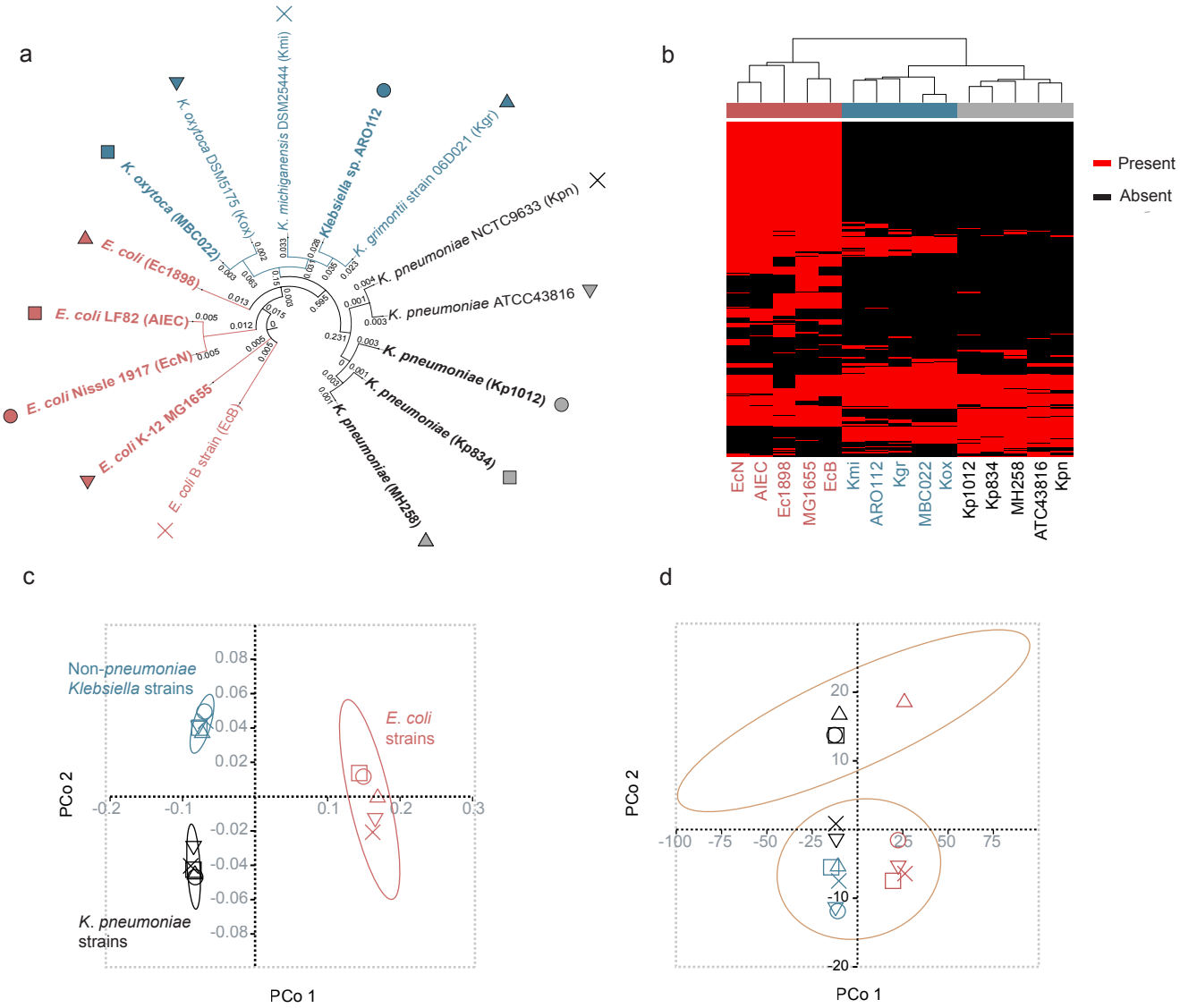
a
K. oxytoca DSM5175 (Kox)
K. michiganensis DSM25444 (Kmi)
Klebsiella sp. ARO112
K. grimontii strain 06D021 (Kgr)
K. oxytoca (MBC022)
K. pneumoniae NCTC9633 (Kpn)
E. coli (Ec1898)
K. pneumoniae ATCC43816
E. coli LF82 (AIEC)
K. pneumoniae (Kp1012)
E. coli Nissle 1917 (EcN)
E. coli K-12 MG1655
K. pneumoniae (Kp834)
E. coli B strain (EcB)
K. pneumoniae (MH258)
b
Present
Absent
EcN
AIEC
Ec1898
MG1655
EcB
Kmi
ARO112
Kgr
MBC022
Kox
Kp1012
Kp834
MH258
ATC43816
Kpn
c
Non-pneumoniae Klebsiella strains
E. coli strains
K. pneumoniae strains
PCo 2
PCo 1
d
PCo 2
PCo 1

Fig. 2

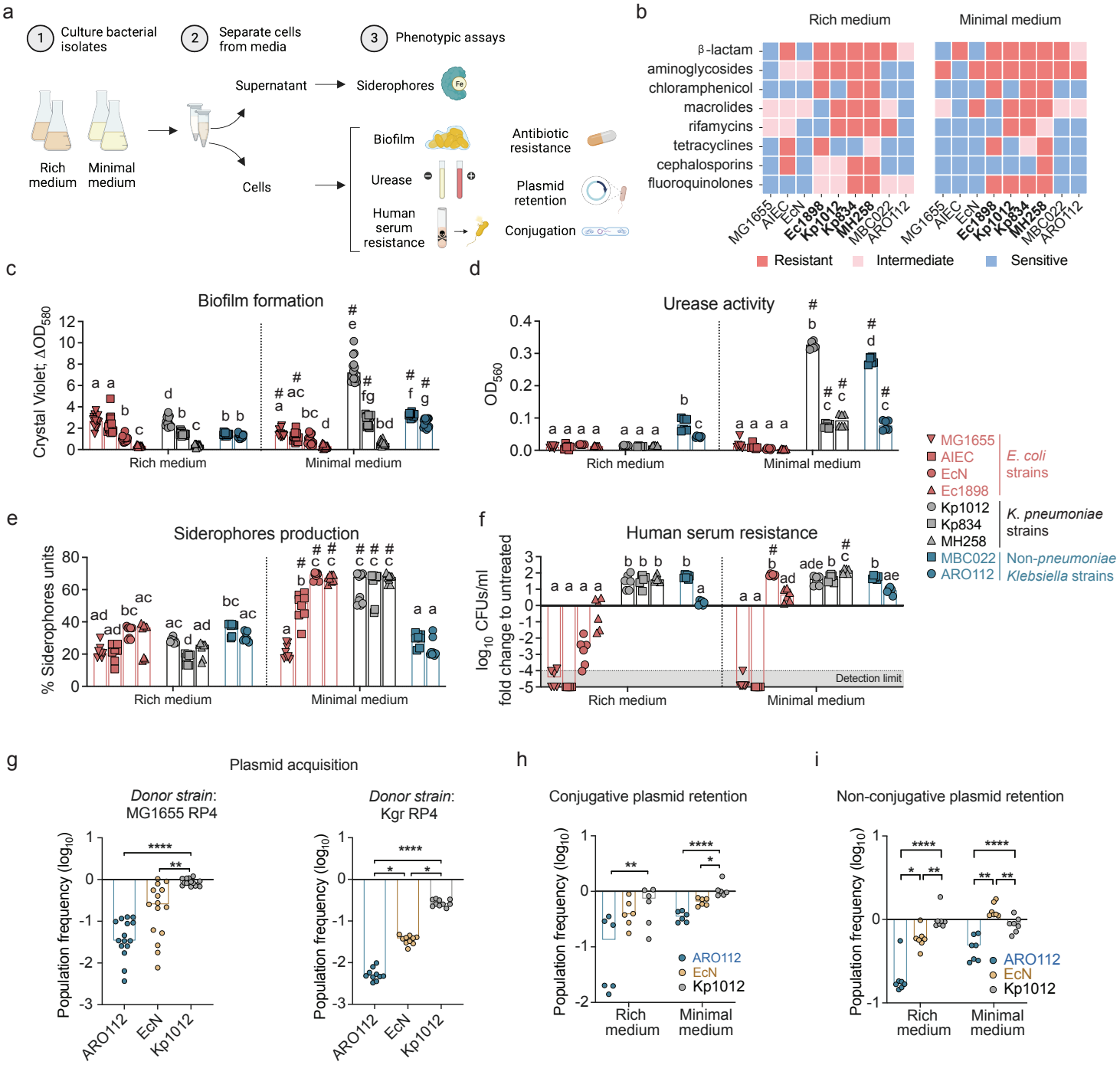
a
1 Culture bacterial isolates
2 Separate cells from media
3 Phenotypic assays
Rich medium
Minimal medium
Supernatant
Siderophores
Cells
Biofilm
Urease
Human serum resistance
Antibiotic resistance
Plasmid retention
Conjugation
b
Rich medium
Minimal medium
β-lactam
aminoglycosides
chloramphenicol
macrolides
rifamycins
tetracyclines
cephalosporins
fluoroquinolones
MG1655
AIEC
EcN
Ec1898
Kp1012
Kp834
MH258
MBC022
ARO112
Resistant
Intermediate
Sensitive
c
Biofilm formation
Crystal Violet, ΔOD580
Rich medium
Minimal medium
d
Urease activity
OD560
Rich medium
Minimal medium
MG1655
AIEC
EcN
Ec1898
E. coli strains
Kp1012
Kp834
MH258
K. pneumoniae strains
MBC022
ARO112
Non-pneumoniae Klebsiella strains
e
Siderophores production
% Siderophores units
Rich medium
Minimal medium
f
Human serum resistance
log10 CFUs/ml fold change to untreated
Detection limit
Rich medium
Minimal medium
g
Plasmid acquisition
Donor strain: MG1655 RP4
Donor strain: Kgr RP4
Population frequency (log10)
ARO112
EcN
Kp1012
h
Conjugative plasmid retention
Population frequency (log10)
ARO112
EcN
Kp1012
Rich medium
Minimal medium
i
Non-conjugative plasmid retention
Population frequency (log10)
ARO112
EcN
Kp1012
Rich medium
Minimal medium

Fig. 3

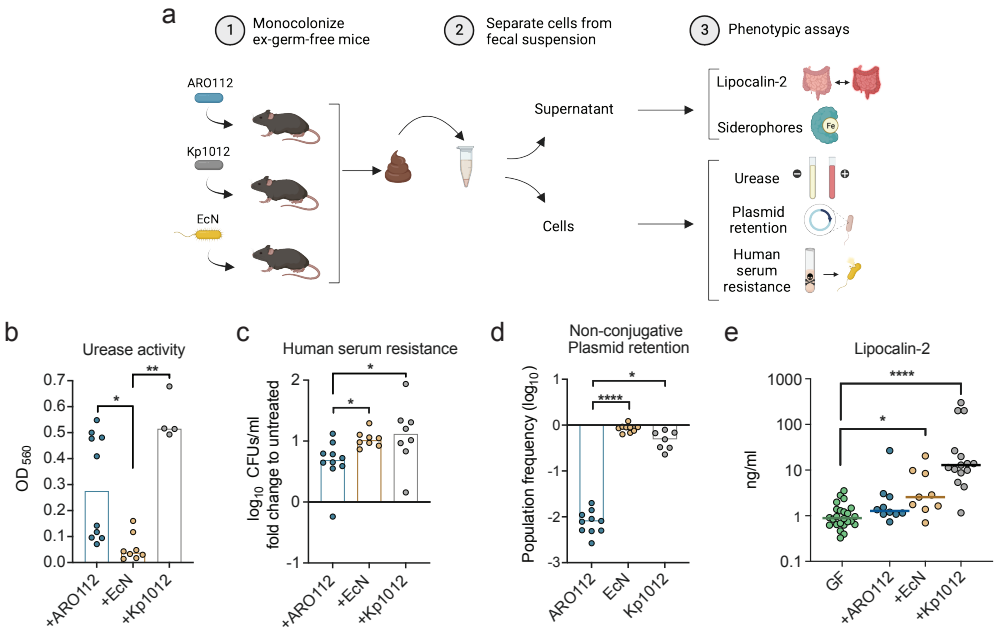
a
1 Monocolonize ex-germ-free mice
2 Separate cells from fecal suspension
3 Phenotypic assays
ARO112
Kp1012
EcN
Supernatant
Cells
Lipocalin-2
Siderophores
Urease
Plasmid retention
Human serum resistance
b
Urease activity
OD 560
+ARO112
+EcN
+Kp1012
c
Human serum resistance
log10 CFUs/ml fold change to untreated
+ARO112
+EcN
+Kp1012
d
Non-conjugative Plasmid retention
Population frequency (log10)
ARO112
EcN
Kp1012
e
Lipocalin-2
ng/ml
GF
+ARO112
+EcN
+Kp1012

Fig. 4

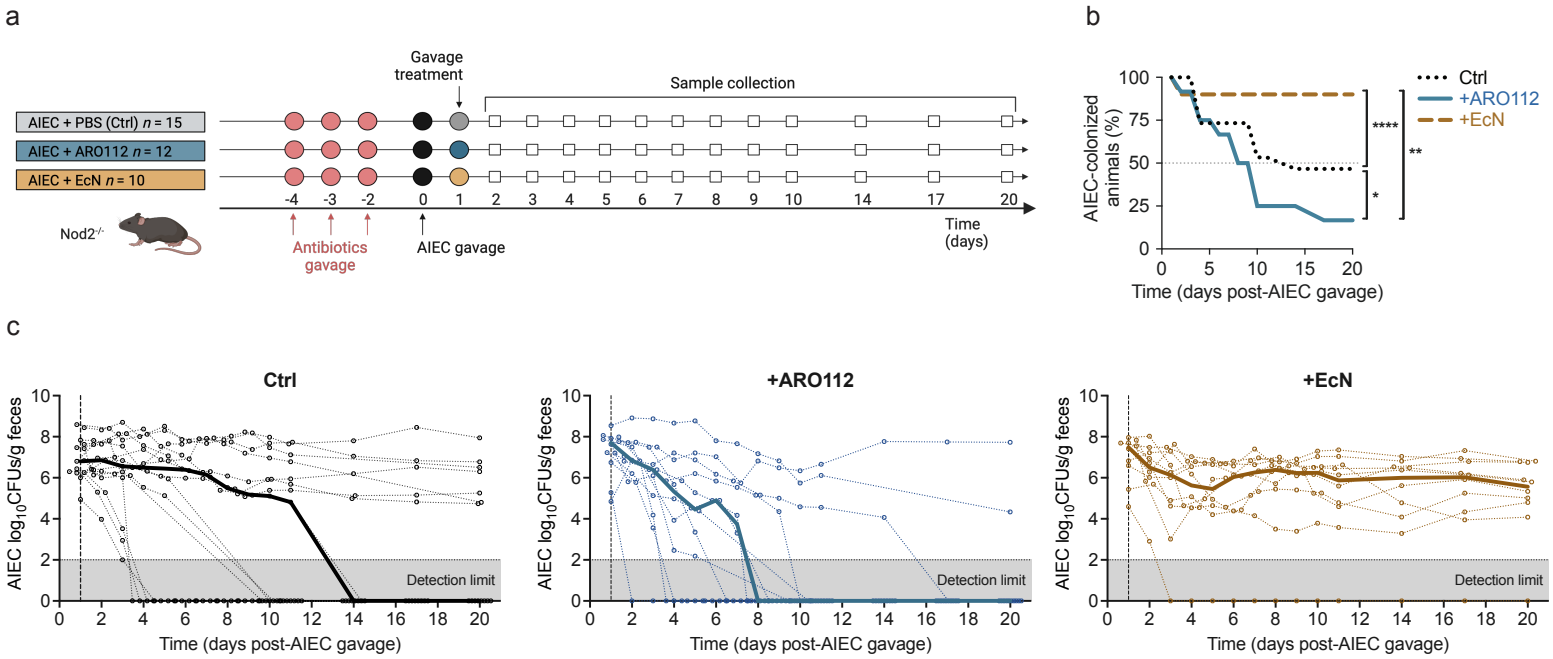
a
Gavage treatment
Sample collection
AIEC + PBS (Ctrl) n = 15
AIEC + ARO112 n = 12
AIEC + EcN n = 10
Nod2-/-
-4 -3 -2 0 1 2 3 4 5 6 7 8 9 10 14 17 20
Antibiotics gavage
AIEC gavage
Time (days)
b
AIEC-colonized animals (%)
Time (days post-AIEC gavage)
Ctrl
+ARO112
+EcN
****
**
*
c
Ctrl
+ARO112
+EcN
AIEC log10CFUs/g feces
Detection limit
Time (days post-AIEC gavage)

Fig. 5

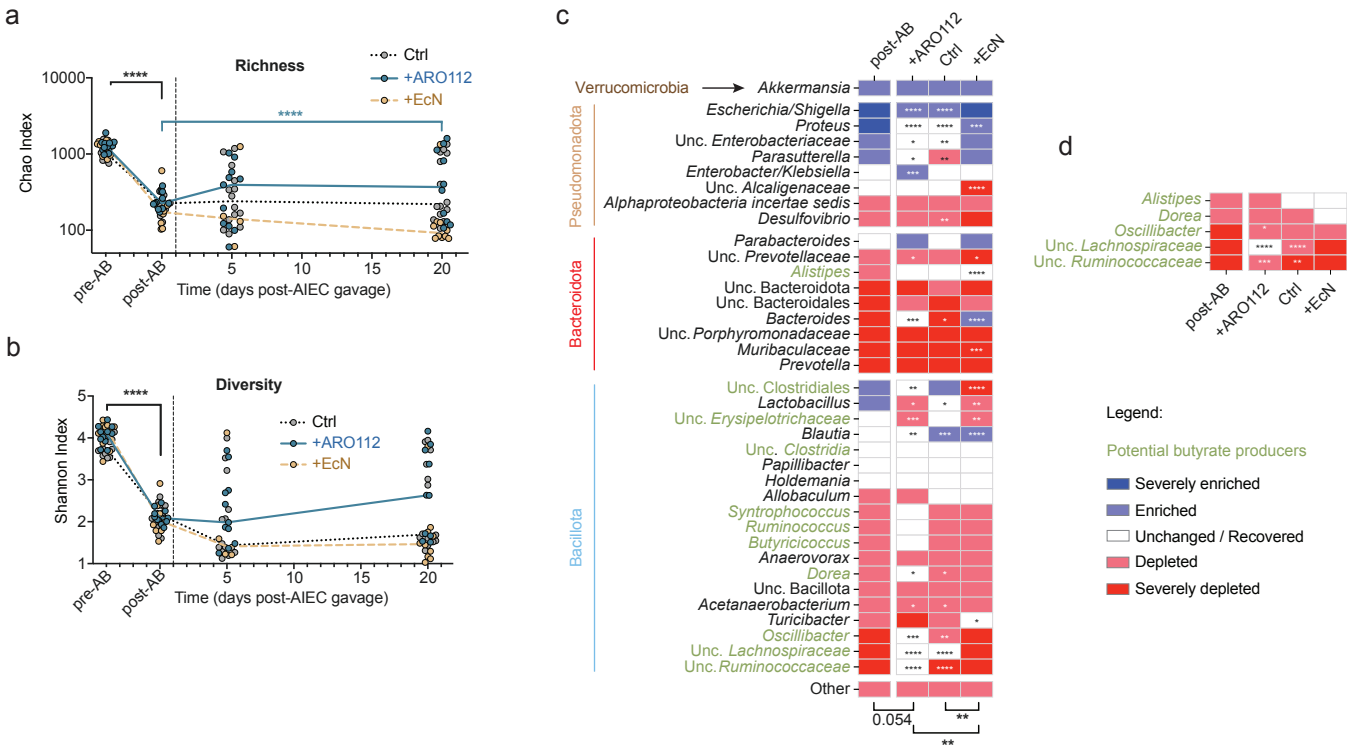
a
Richness
Ctrl
+ARO112
+EcN
Chao Index
10000
1000
100
****
****
pre-AB
post-AB
5
10
15
20
Time (days post-AIEC gavage)
b
Diversity
Shannon Index
5
4
3
2
1
****
Ctrl
+ARO112
+EcN
pre-AB
post-AB
5
10
15
20
Time (days post-AIEC gavage)
c
post-AB
+ARO112
Ctrl
+EcN
Verrucomicrobia
Akkermansia
Pseudomonadota
Escherichia/Shigella
Proteus
Unc. Enterobacteriaceae
Parasutterella
Enterobacter/Klebsiella
Unc. Alcaligenaceae
Alphaproteobacteria incertae sedis
Desulfovibrio
Bacteroidota
Parabacteroides
Unc. Prevotellaceae
Alistipes
Unc. Bacteroidota
Unc. Bacteroidales
Bacteroides
Unc. Porphyromonadaceae
Muribaculaceae
Prevotella
Bacillota
Unc. Clostridiales
Lactobacillus
Unc. Erysipelotrichaceae
Blautia
Unc. Clostridia
Papillibacter
Holdemania
Allobaculum
Syntrophococcus
Ruminococcus
Butyricicoccus
Anaerovorax
Dorea
Unc. Bacillota
Acetanaerobacterium
Turicibacter
Oscillibacter
Unc. Lachnospiraceae
Unc. Ruminococcaceae
Other
0.054
**
**
d
Alistipes
Dorea
Oscillibacter
Unc. Lachnospiraceae
Unc. Ruminococcaceae
post-AB
+ARO112
Ctrl
+EcN
Legend:
Potential butyrate producers
Severely enriched
Enriched
Unchanged / Recovered
Depleted
Severely depleted

Fig. 6

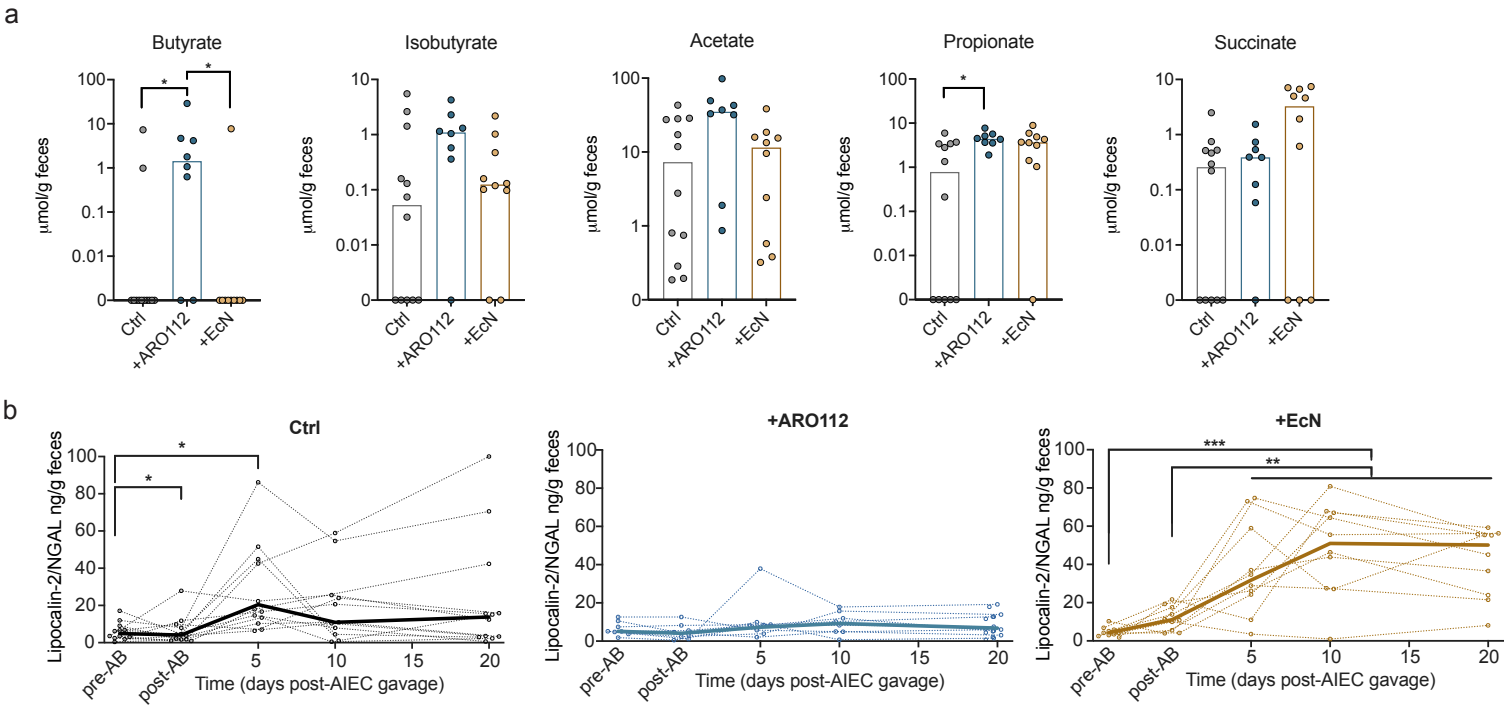
a
Butyrate
Isobutyrate
Acetate
Propionate
Succinate
µmol/g feces
Ctrl
+ARO112
+EcN
b
Ctrl
+ARO112
+EcN
Lipocalin-2/NGAL ng/g feces
pre-AB
post-AB
Time (days post-AIEC gavage)

Extended Data Fig. 1

a

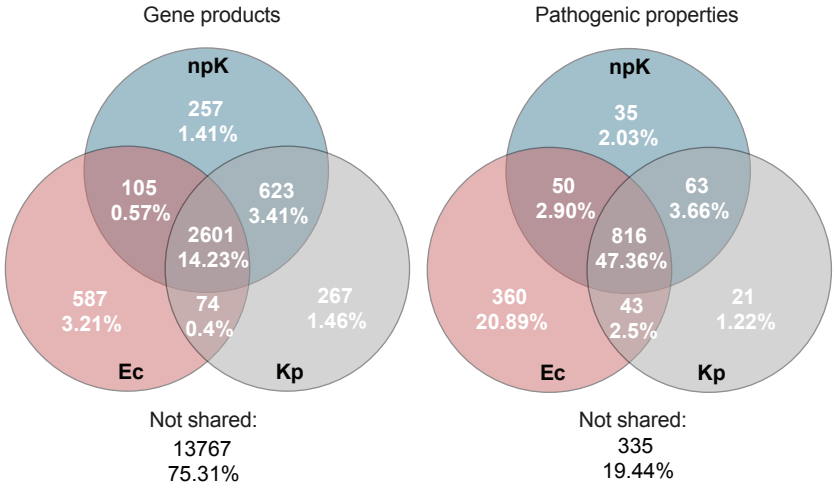

b

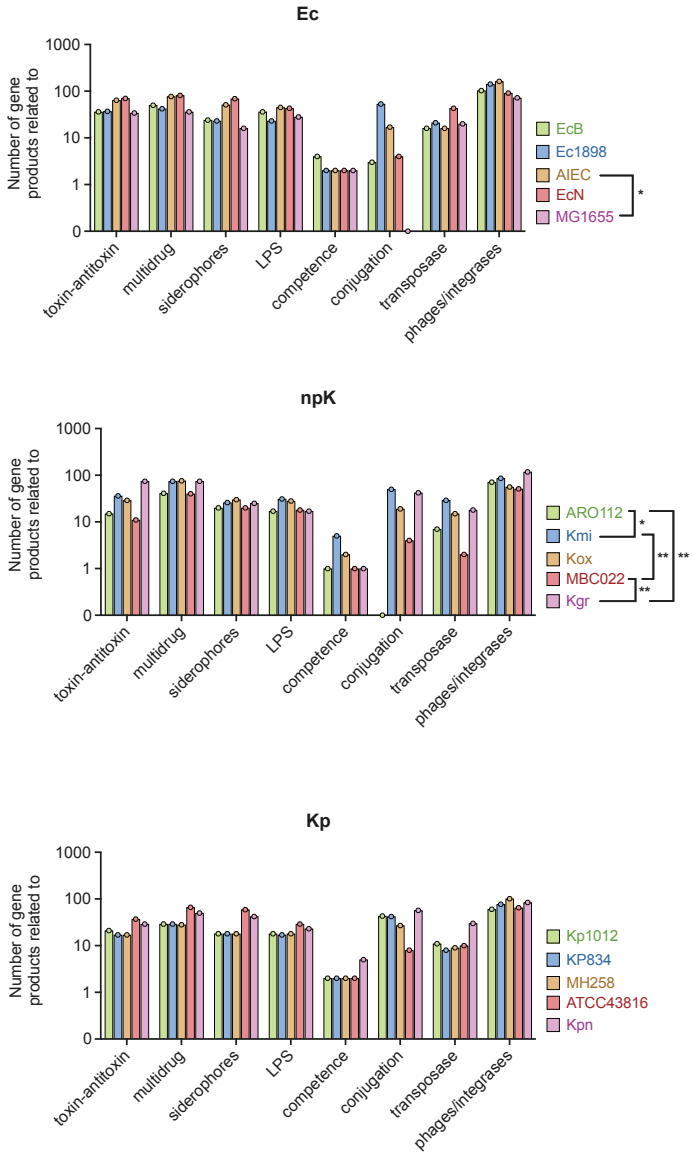

Extended Data Fig. 2

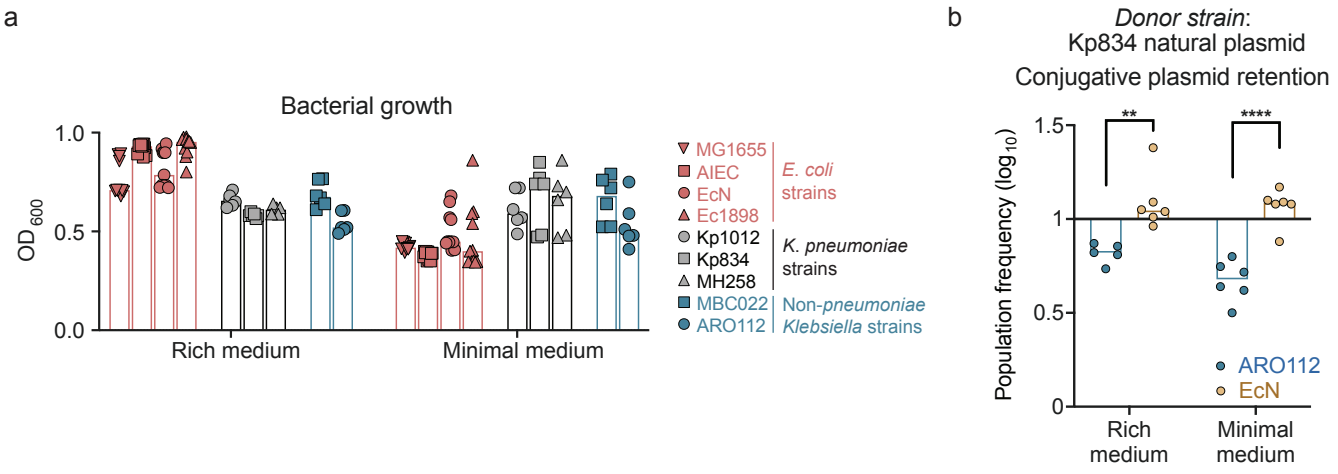

Extended Data Fig. 3

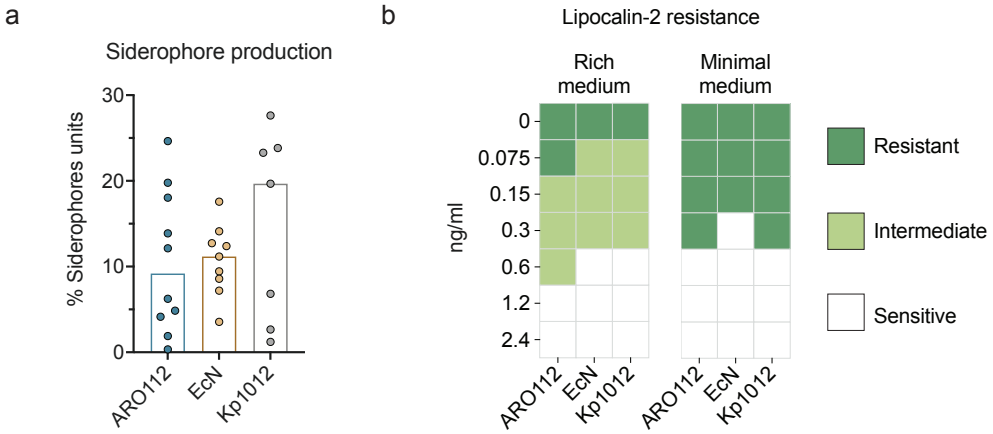

Extended Data Fig. 4

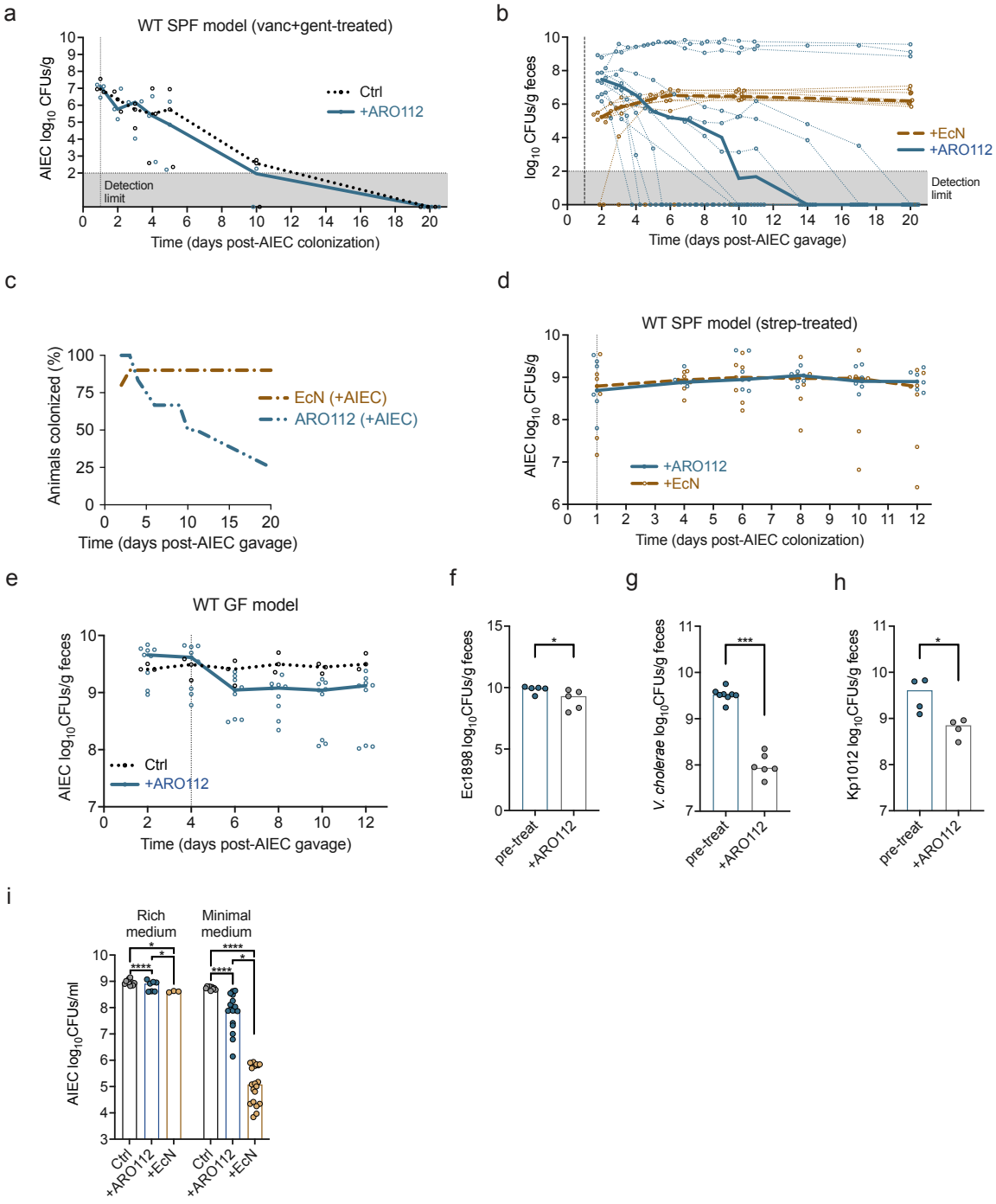

Extended Data Fig. 5

a

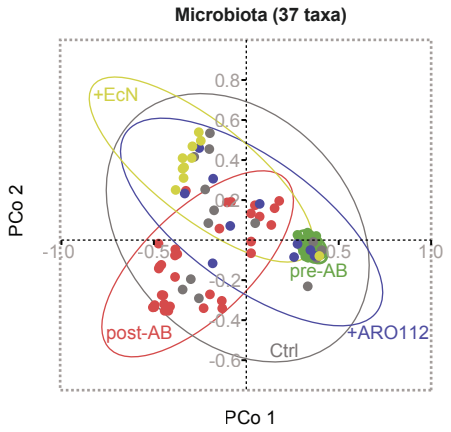

b

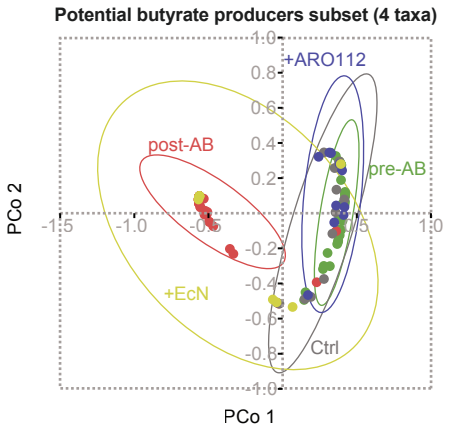
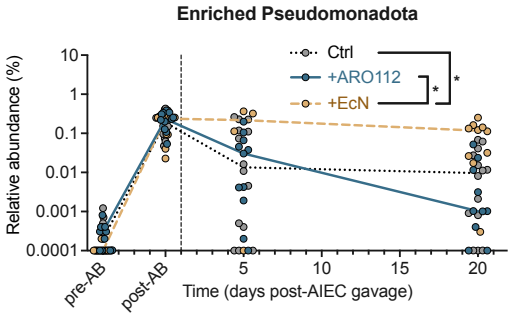
c